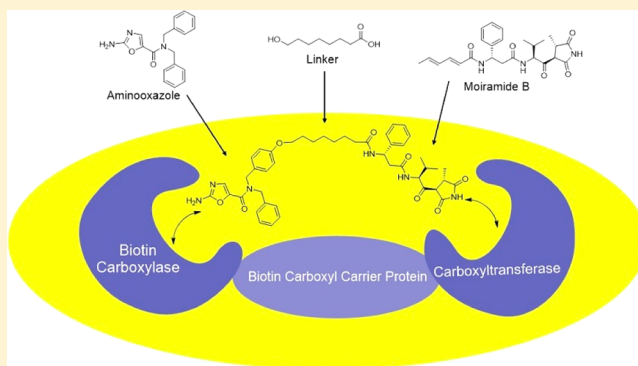


Design, Synthesis, and Antibacterial Properties of Dual-Ligand Inhibitors of Acetyl-CoA Carboxylase

Molly A. Silvers,[†] Gregory T. Robertson,[‡] Carol M. Taylor,[§] and Grover L. Waldrop^{*,†}[†]Division of Biochemistry and Molecular Biology, Louisiana State University, Baton Rouge, Louisiana 70803, United States[‡]Department of Microbiology, University of Texas Southwestern Medical Center, Dallas, Texas 75390, United States[§]Department of Chemistry, Louisiana State University, Baton Rouge, Louisiana 70803, United States

Supporting Information

ABSTRACT: There is an urgent demand for the development of new antibiotics due to the increase in drug-resistant pathogenic bacteria. A novel target is the multifunctional enzyme acetyl-CoA carboxylase (ACC), which catalyzes the first committed step in fatty acid synthesis and consists of two enzymes: biotin carboxylase and carboxyltransferase. Covalently attaching known inhibitors against these enzymes with saturated hydrocarbon linkers of different lengths generated dual-ligand inhibitors. Kinetic results revealed that the dual-ligands inhibited the ACC complex in the nanomolar range. Microbiology assays showed that the dual-ligand with a 15-carbon linker did not exhibit any antibacterial activity, while the dual-ligand with a 7-carbon linker displayed broad-spectrum antibacterial activity as well as a decreased susceptibility in the development of bacterial resistance. These results suggest that the properties of the linker are vital for antibacterial activity and show how inhibiting two different enzymes with the same compound increases the overall potency while also impeding the development of resistance.



INTRODUCTION

In 2013, the U.S. Centers for Disease Control and Prevention (CDC) issued an alarming report on the dramatic rise in antibiotic-resistant bacteria.¹ The report noted that in the U.S., over 2 million people per year are afflicted with bacterial infections that are resistant to at least one antibiotic. In addition, there are 23 000 deaths per year directly attributable to antibiotic-resistant infections. One of the core recommendations in the report for combating this public health crisis is the development of new antibiotics. The current arsenal of antibiotics is directed at only 30–40 molecular targets. Thus, there is a pressing need to develop antibiotics against novel targets. Fatty acid biosynthesis is an essential metabolic pathway in both eukaryotes and prokaryotes, and since fatty acids are required for membrane biogenesis in bacteria, fatty acid synthesis is an attractive pathway to focus on for antibiotic development.^{2–4}

The first committed and regulated reaction in fatty acid biosynthesis is catalyzed by the multifunctional enzyme acetyl-CoA carboxylase (ACC).⁵ The overall reaction catalyzed by ACC is shown in Scheme 1. ACC requires the vitamin biotin, which is covalently attached to the biotin carboxyl carrier protein (BCCP). In the first half-reaction, catalyzed by biotin carboxylase (BC), BCCP-biotin is carboxylated in an ATP-dependent manner where bicarbonate is the source of CO₂. The second half-reaction, catalyzed by carboxyltransferase

(CT), involves the transfer of the carboxyl group from BCCP-biotin to acetyl-CoA to form malonyl-CoA. In eukaryotes, the three proteins that comprise ACC form domains on a single polypeptide chain,⁶ whereas in prokaryotes, they are encoded as three separate proteins.⁷ The bacterial forms of BC and CT retain their activity when isolated from the other components and can utilize free biotin as a substrate.^{4,5} With respect to antibacterial development, the different arrangement of the three protein components of ACC between eukaryotes and prokaryotes provides potential for the design of inhibitors that selectively target the bacterial system.^{3,4} Moreover, the three components of ACC are highly conserved among bacterial species, increasing the likelihood of developing broad spectrum antibacterial agents.^{7,8}

Both the BC and the CT components of ACC have served as targets for antibacterial agents. Miller et al. discovered that the antibacterial properties of the pyridopyrimidine class of molecules was due to the inhibition of BC.⁹ The pyridopyrimidines (e.g., compound 1, Figure 1) bound in the ATP binding site of bacterial BC but did not inhibit human BC. The pyridopyrimidines were not readily amenable to synthetic modifications, so Mochalkin et al. used fragment and virtual screening to identify a series of amino-oxazole derivatives (e.g.,

Received: July 17, 2014

Scheme 1. Reactions Catalyzed by Acetyl-CoA Carboxylase

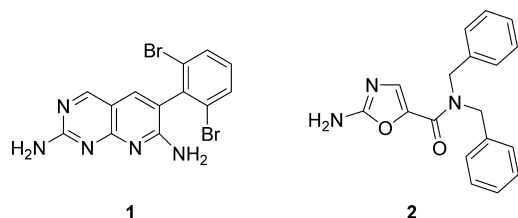
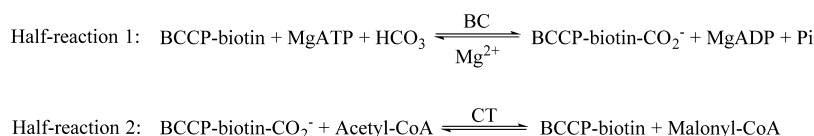


Figure 1. Pyridopyrimidine **1** and aminooxazole **2**, inhibitors of biotin carboxylase.

compound **2** in Figure 1) that also inhibited BC by binding in the ATP binding site.¹⁰ In common with the pyridopyrimidines, the aminooxazole derivatives were selective inhibitors of the bacterial, but not human, BC.¹⁰

In contrast to BC, there is only one known class of molecules that inhibits the CT component of ACC and also possesses antibacterial activity. While the BC inhibitors are invariably of synthetic origin, the CT inhibitors are natural products. The antibacterial activity of andrimid and moiramide B (**3** and **4**, respectively, Figure 2) displayed broad spectrum activity.¹¹

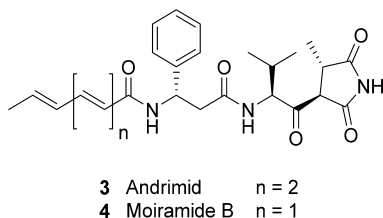


Figure 2. Andrimid (**3**) and moiramide B (**4**), inhibitors of carboxyltransferase.

Their antibacterial activity had been known for at least 10 years before Freiberg et al. discovered that the molecular target for andrimid and moiramide B was the CT subunit of ACC.^{11,12} Structure–activity relationship (SAR) studies revealed that the pyrrolidinedione headgroup was essential for enzyme inhibition and antibacterial activity, while the fatty acid chain is not required.¹³ Compound **4** was found to have an inhibition constant of 5 nM and exhibited competitive inhibition versus malonyl-CoA.^{12,14} Compound **4** inhibited CT from both Gram-negative and Gram-positive organisms, which is consistent with its broad spectrum activity. In common with the BC inhibitors, **4** did not inhibit human ACC.¹²

Despite the fact that both BC and CT have been validated as unique targets for antibacterial development through the discovery of selective antibacterial inhibitors, both targets suffer from high potential for spontaneous resistance through individual target-based mutations. One approach to decrease the likelihood of developing resistance is to make a single molecule that incorporates inhibitory motifs for both the BC and CT enzymatic activities. The potential lower frequency of resistance against such a dual-ligand inhibitor is explained by considering the genetic arrangement of ACC. Biotin carboxylase is a homodimer encoded by the *accC* gene, while

carboxyltransferase is a heterotetramer with α - and β -subunits encoded by *accA* and *accD*, respectively. The *accA* and *accD* genes encoding the subunits of CT are not genetically linked.¹⁵ This genetic arrangement is commonly found in both Gram-negative and Gram-positive bacteria. Thus, one would predict that nonessential missense mutations would have to arise in three different genes in order for the bacteria to become resistant to a molecule targeting both enzymes simultaneously.

While the use of dual-ligands for lowering the frequency of resistance is well documented,^{16–19} most examples of dual-ligands as antibacterial agents involve inhibitors that target two enzymes that either do not interact and/or are not related metabolically. Thus, a dual-ligand inhibitor of ACC would represent a departure from previous practice. In fact, a dual-ligand inhibitor of ACC is a particularly attractive strategy for inhibition of the enzyme in light of recent studies that have demonstrated that all three protein components (BC, BCCP, and CT) must form a complex in vivo for activity.²⁰ On this background, we report the first step toward dual-ligand inhibition of ACC by covalently linking the BC inhibitory motif of compound **2** to the core structure of compound **4**, that exhibits CT inhibition, and characterizing the inhibitory and antibacterial properties.

RESULTS AND DISCUSSION

Design Strategy. In order to generate dual-ligand inhibitors incorporating these known inhibitory motifs, we needed to identify loci in each inhibitor where we could attach a metabolically stable linker without compromising binding and biological activity. A suitable, stable functional group needed to be placed on the dibenzylamide moiety of **2** (Figure 1). We decided to incorporate a hydroxyl group at the *para* position of one of the benzene rings with the potential for etherification. This modification was not expected to affect binding to BC, since it is the aminooxazole moiety that is responsible for interaction with the ATP binding site.¹⁰ In the case of moiramide B (compound **4**, Figure 2), it has been shown that the fatty acid side chain can be significantly modified with retention of biological activity.¹³ We thereby elected to replace this fatty acid chain with a lipophilic linker at the *N*-terminus of the β -phenylalanine residue in the naturally occurring, biologically active pseudopeptide. These design features gave rise to dual-ligands **5** and **6** (Figure 3).

Finally, we needed to choose linkers to covalently connect the aminooxazole and moiramide components of the dual-ligand inhibitor. The most important criterion for the linker segment was stability. Intracellular degradation of the linker segment would lead to the false conclusion that dual-ligands directed against ACC were not feasible as antibacterial agents. While a variety of chemical constructs could serve as the linker segment, a saturated hydrocarbon was selected because it was least susceptible to intracellular degradation and would afford the best chance for determining the feasibility of the dual-ligand hypothesis for ACC.

We chose a saturated aliphatic compound with a leaving group at one end, to form an ether with the phenol at the

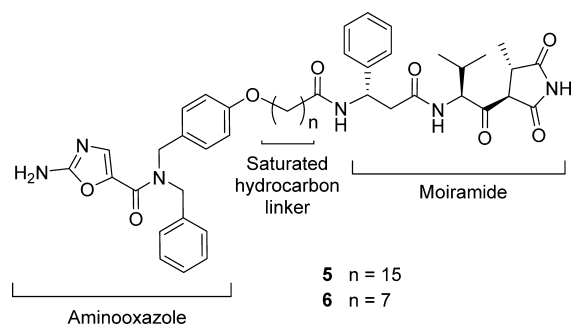


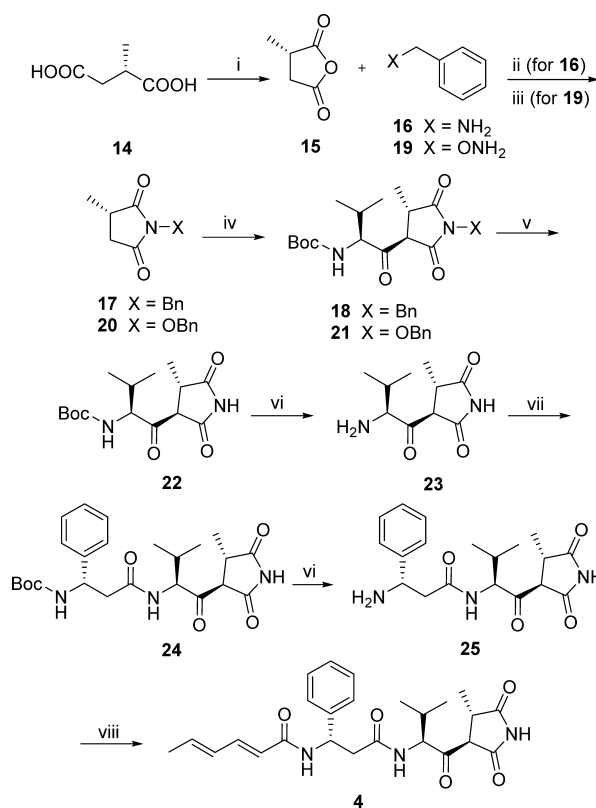
Figure 3. Dual-ligand inhibitors containing aminooxazole and moiramide pharmacophores with saturated hydrocarbon linkers with 15-carbons (compound 5) and 7-carbons (compound 6).

“aminooxazole end”, and a carboxylic acid at the other end to form an amide with the *N*-terminus of the moiramide fragment. We arbitrarily started with a 15-carbon linker since juniperic acid (compound 26, see Scheme 4, below) is commercially available. We later also utilized a 7-carbon linker (from 8-hydroxyoctanoic acid, see Scheme 4) to more accurately mimic the fatty acid component of moiramide B. This design strategy generates dual-ligand inhibitors that incorporate the necessary pharmacophores for targeting both BC and CT while covalently attaching them using stable, saturated hydrocarbon linkers of various lengths (Figure 3).

Chemistry. We generated the requisite unsymmetrical dibenzylamine via reductive amination of benzaldehyde with *p*-aminophenol to give compound 10 (Scheme 2).²¹ Coupling of carboxylate 12 with secondary amine 10 afforded compound 13 (Scheme 2), the “aminooxazole” component of the dual-ligand inhibitor, with a handle for attachment to other species.¹⁰ However, compound 2 was also synthesized and used in biological studies as the “aminooxazole only” representative in order to eliminate any side reactions that might have been encountered with the phenol functionality of 13.

Compounds 3 and 4 have been synthesized previously, although most reports are in communication format without experimental details.^{13,22–24} These accounts all alluded to the fragility of the β -ketoamide functionality; the pK_a for enolate formation of andrimid is 6.8.²⁵ We prepared anhydride 15 (Scheme 3) from commercially available (4*S*)-methyl-succinic acid according to Midgley and Thomas²⁶ and converted this to

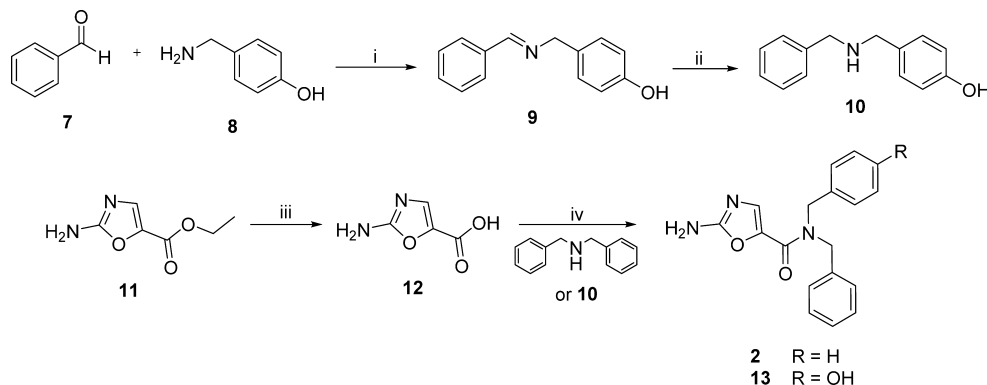
Scheme 3. Synthesis of Amine 25 and Compound 4^a



^aReagents and conditions: (i) $AcCl$, 60 °C, 97%; (ii) 1. Compound 16, THF, Δ ; 2. Ac_2O , Δ , 83%; (iii) Compound 19, CDI, triethylamine, CH_2Cl_2 , 89%; (iv) 1. *N*-Boc-L-valine, CDI, dry THF; 2. LiHMDS, -78 °C, dry THF, 42%; (v) 1. H_2 , 5% Pd/C (20% w/w), dry methanol; 2. 2-bromoacetophenone, triethylamine, CH_3CN , 64%; (vi) TFA: CH_2Cl_2 , 0 °C, 89–98%; (vii) (*S*)-*N*-Boc-3-amino-3-phenylpropanoic acid, HATU, iPr_2NEt , dry DMF, 0 °C to rt, 45%; (viii) Sorbic acid, TBTU, iPr_2NEt , dry DMF, 32%.

the benzyl protected succinimide 17.²⁷ Indeed, Pohlmann et al. had prepared a number of *N*-alkylated derivatives of moiramide for SAR studies but they did not prepare the benzyl derivative, and it was not clear why they and others used benzyloxy protection for the succinimide nitrogen, which requires two

Scheme 2. Synthesis of Aminooxazole 2 and Aminooxazole 13 with a *para*-Hydroxyl Group^a



^aReagents and conditions: (i) triethylamine, dry methanol, 3 Å molecular sieves, 65%; (ii) $NaBH_4$, dry methanol, 0 °C to rt, 84%; (iii) 1. 2 M NaOH, 60 °C; 2. HCl, 98%; (iv) HATU, triethylamine, dry DMF, 31–35%.

steps for removal. We expected to cleave the benzylamine in a single hydrogenolytic step.

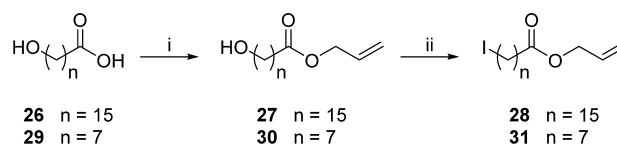
We now faced the challenging acylation of the kinetic enolate of **17** with an acyl cation equivalent derived from *N*-tert-butoxycarbonyl-L-valine (Boc-Val-OH). The discussion by Davies and Dixon informed us that the enolate was unstable and must be generated in the presence of an appropriate electrophile.²⁴ While they employed an *N*-carboxyanhydride, others invoked an acyl imidazole.^{13,23} We found the acyl imidazole was more convenient to generate and more stable than the *N*-carboxyanhydride. The acyl imidazole generated from Boc-Val-OH was added to a solution of compound **17**. The solution was added slowly to a solution of LiHMDS in THF at -78 °C. While TLC analysis of the reaction looked promising, poor yields of compound **18** were obtained by flash chromatography. Two-dimensional TLC confirmed that **18** was unstable to silica gel and was thus isolated by reversed-phase HPLC in low yield. Furthermore, the product was not particularly stable, and standard hydrogenolysis procedures for removing the benzyl protecting group were unsuccessful.

The *N*-benzyl group was replaced with the *N*-benzyloxy protecting group, ultimately leading to compound **21** (Scheme 3) that was remarkably stable to silica gel. An earlier paper by Robin et al., outlining a synthesis of thalidomide, also utilized benzyloxy protection of the glutarimide ring, where the benzyl group had been problematic.²⁸ They suggested that resonance donation of electron density from the oxygen reduces the electrophilicity of the C=O groups and the acidity of the neighboring alpha protons. The acylation of **20** and purification of **21** was now realized in a better yield of 42%, and the product was stable, albeit as an equilibrium mixture of predominantly the *trans* diastereomer and <10% of the diastereomer with *cis*-relative stereochemistry on the succinimide ring that arises via tautomerization to the enol form, evident in <6%. Earlier reports did not include NMR spectra, although Davies and Dixon reported an 87:9:4 (*trans*:enol:*cis*) mixture for compound **21**. The benzylic C–O bond in **21** was cleaved by hydrogenolysis to afford the hydroxylamine that was treated with 2-bromoacetophenone to generate the phenacyl ester *in situ* which ultimately led to succinimide **22**.²⁴ The deprotected succinimide **22** existed as an 82:4:14 (*trans*:enol:*cis*) mixture; Davies and Dixon did not report a ratio of isomers for this compound. Removal of the Boc group at the *N*-terminus of compound **22** and elongation with commercially available Boc- β -Phe-OH gave compound **24**. The addition of the Boc- β -Phe moiety resulted in a single diastereomer, suggesting a stronger thermodynamic preference for the *trans* isomer with the larger acyl side chain. Compound **24** in turn underwent Boc deprotection to afford the free amine **25** that was coupled to sorbic acid to generate compound **4** (Scheme 3).

Preparation of the 15-carbon linker followed a procedure that Overman and co-workers had previously reported for the conversion of acid **26** to allyl ester **27** (Scheme 4).²⁹ The primary alcohol was converted to alkyl iodide **28** by analogy to a procedure of Jobron et al.³⁰ We also prepared a significantly shorter linker, viz. **31**, as shown in Scheme 4.

The convergent assembly of the three fragments to generate the dual-ligand inhibitors is depicted in Scheme 5. The phenol of compound **13** was activated as the corresponding cesium salt using CsOH. This accentuated nucleophile then participated in an S_N2 reaction with the iodide of compounds **28** and **31** to generate an ether linkage, viz. aminoazazole-linker conjugates **32** and **33**, respectively. The allyl protecting group of each

Scheme 4. Synthesis of Modified Saturated Hydrocarbon Linkers **28** and **31**^a

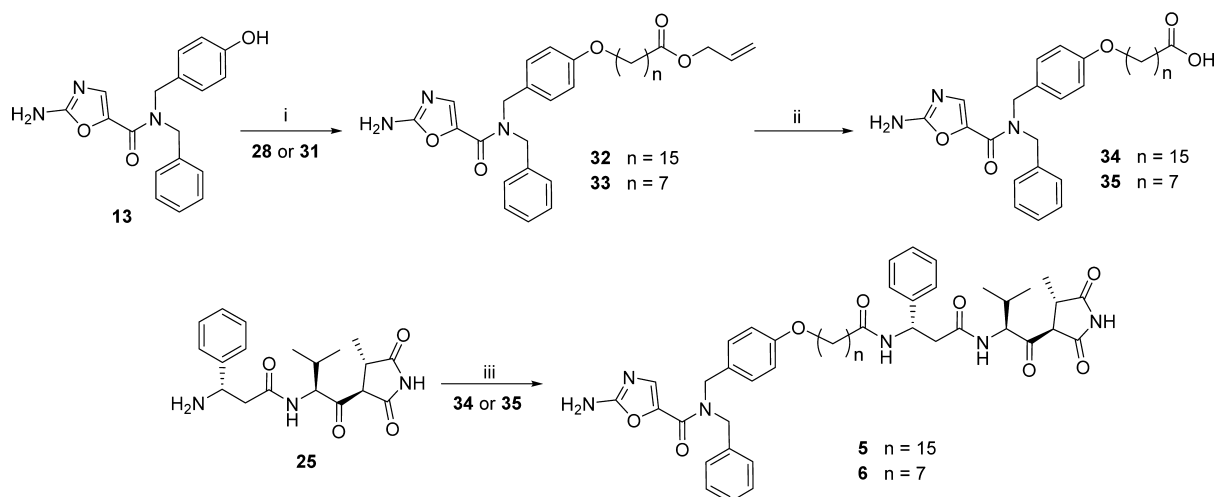


^aReagents and conditions: (i) allyl alcohol, H₂SO₄, heat, 59–61%; (ii) polymer-bound triphenylphosphine, I₂, imidazole, dry CH₂Cl₂, 78–83%.

derivative was removed by hydrolysis to generate the free carboxylic acids **34** and **35**, by a procedure analogous to one of Zhang et al.³¹ The acids were each coupled to the amine in compound **25** using standard coupling reagents to generate compounds **5** and **6** that were purified by RP-HPLC.¹³ Using an Agilent Zorbax Stable Bond-C18 column, compound **6** (7C linker) eluted as expected, but compound **5** (15C linker) was retained, most likely due to the increased hydrophobicity of **5**. Fortunately, the use of an Agilent Zorbax Extend-C18 column with double end-capping allowed for the elution and purification of **5** (Scheme 5).

Inhibition of Acetyl-CoA Carboxylase by the Dual-Ligands. The targets of the antibacterial agents **2** and **4** are BC and CT, respectively. The question now is how would a molecule that incorporates the features of both compounds **2** and **4** inhibit the multiprotein complex comprising all three components of ACC? Recent studies have shown that the three components of ACC—BC, BCCP, and CT—form a multiprotein complex both *in vitro* and *in vivo*.²⁰ In order to compare the dual-ligand inhibitors to the two parent compounds, the inhibition of ACC by compounds **2** and **4** was also studied because the original characterization of these inhibitors utilized only the isolated subunits of BC or CT, not the ACC complex.

The inhibition of ACC by compound **2** was determined by varying ATP at increasing fixed concentrations of inhibitor, where acetyl-CoA was held constant at a subsaturating level. Compound **2** exhibited noncompetitive inhibition versus ATP with a K_{is} of 0.4 ± 0.1 μM and a K_{ii} of 0.9 ± 0.2 μM (Figure 4A). In fact, even at 9 times the K_m value for ATP (56 μM), compound **2** was still able to inhibit the activity of the enzyme. This pattern was unexpected based on the competitive inhibition versus ATP that was observed with the isolated subunit of BC (Supporting Information, Figure S1). However, the K_{is} of 0.8 ± 0.2 μM for isolated BC was close to the K_{is} value observed for ACC. The reason for the noncompetitive pattern in ACC is not clear at this time and awaits the determination of the three-dimensional structure of ACC bound to **2**. Nonetheless, the noncompetitive inhibition pattern observed for ACC has implications for targeting the BC subunit of the enzyme for pharmaceutical purposes. Namely, the noncompetitive inhibition pattern means that inhibitor binding is not precluded by saturating levels of ATP. The K_m for ATP in ACC is reported to be 1–2 μM ,²⁰ however, we consistently measured a K_m value of 6 μM . Nevertheless, the intracellular level of ATP in log phase *Escherichia coli* is 9 mM,³² therefore, ACC is very likely saturated with the substrate ATP *in vivo*. Thus, at least for the BC inhibitor (compound **2**), saturation with ATP will not be problematic. These results show that it is imperative that any potential antibacterial agents targeting either the BC or CT subunits of ACC must be characterized

Scheme 5. Synthesis of Compounds 5 and 6^a

^aReagents and conditions: (i) 1. CsOH, dry DMF; 2. Compounds 28 or 31, dry THF, Δ , 20–21%; (ii) 2 M NaOH, MeOH:THF, 71–89%; (iii) Compound 34 or 35, HATU, Pr_2NEt , dry DMF, 0 °C to rt, 17–19%.

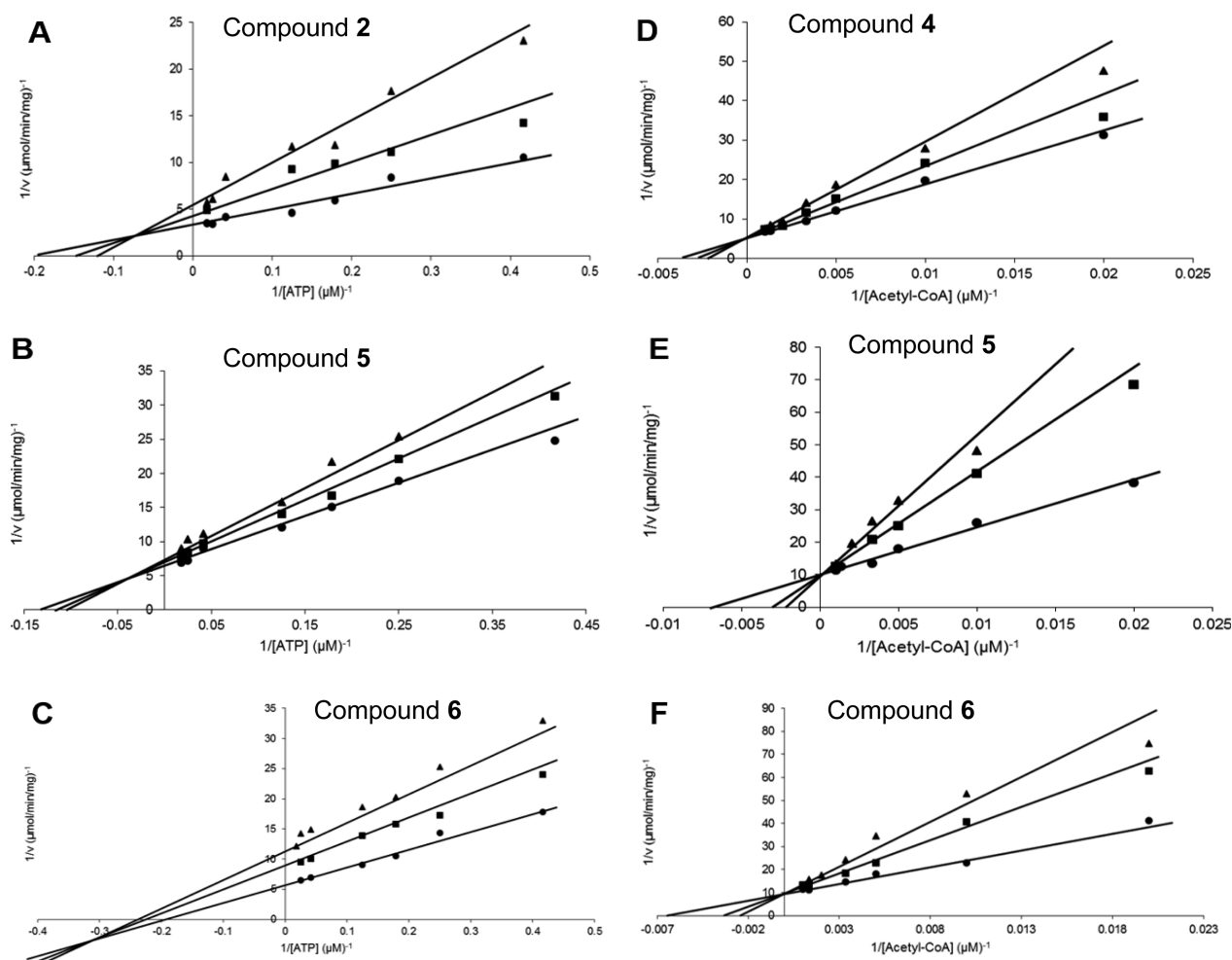


Figure 4. Inhibition of acetyl-CoA carboxylase. (A) Inhibition by 2 at 0 (\bullet), 0.3 (\blacksquare), and 0.7 μM (\blacktriangle). (B) Inhibition by 5 at 0 (\bullet), 6 (\blacksquare), and 10 nM (\blacktriangle). (C) Inhibition by 6 at 0 (\bullet), 6 (\blacksquare), and 10 nM (\blacktriangle). For all three assays, the substrate ATP was varied from 0.4 to 9.0 times the K_m value for ATP. The other substrates, HCO_3^- and acetyl-CoA, were held constant at 15 mM and 200 μM , respectively. The points represent the observed velocities, and the lines represent the best fit of the data to eq 2. (D) Inhibition by 4 at 0 (\bullet), 3 (\blacksquare), and 6 nM (\blacktriangle). (E) Inhibition by 5 at 0 (\bullet), 6 (\blacksquare), and 10 nM (\blacktriangle). (F) Inhibition by 6 at 0 (\bullet), 6 (\blacksquare), and 10 nM (\blacktriangle). For all three assays, the substrate acetyl-CoA was varied while the other substrates, HCO_3^- and ATP, were held constant at 15 mM and 5 μM , respectively. The points represent the observed velocities, and the lines represent the best fit of the data to eq 1.

Table 1. Antibacterial Activities of Synthesized Compounds against Strains of Bacteria

strain (genotype) ^a	MIC ^b (μg/mL)							
	rifampin	gentamicin	chloramphenicol	kanamycin	2	4	5	6
<i>P. aeruginosa</i> (wild-type)	31	2	>64	128	>64	>64	>64	>64
<i>P. aeruginosa</i> (ΔRND) ^c	31	0.5	2	64	>64	8	>64	>64
<i>E. coli</i> (wild-type)	31	0.1	8	2	>64	>64	>64	>64
<i>E. coli</i> (<i>lpxC101</i>)	0.06	0.12	4	1	>64	4	>64	>64
<i>E. coli</i> (<i>tolC</i>)	8	0.24	1	2	16	0.5	>64	8
<i>E. coli</i> (<i>tolC</i> , moir-R) ^d	ND	ND	ND	0.5	8	4	ND	16
<i>E. coli</i> (<i>lpxC101</i> , <i>tolC</i>) ^d	0.5	≤0.03	1	0.5	16	0.5	>64	4
<i>S. aureus</i> (wild-type)	≤0.03	0.5	8	4	>64	1	>64	4
<i>S. aureus</i> (moir-R)	ND	ND	ND	2	>64	8	ND	>64
<i>S. aureus</i> (<i>norA</i> ^{up})	≤0.03	0.5	8	4	>64	4	>64	4
<i>S. epidermidis</i> (wild-type)	≤0.03	8	8	>128	>64	0.24	>64	1
<i>E. faecalis</i> (wild-type)	0.5	8	8	31	>64	8	>64	4

^aThe following designate targeted deletion mutants of efflux pumps or subunits of efflux pumps: *mexAB*, *mexCD*, *mexXY*, *mexHI*, *opmH*, *tolC*. The *lpxC101* allele enhances permeability of the *E. coli* outer membrane. The *norA*^{up} genotype results from a spontaneous mutation in *S. aureus* resulting in a gain of function of the *norA* efflux pump. The designation moir-R indicates a spontaneous moiramide resistance selected with moiramide B containing agar at 4–8 times the MIC. Wild-type *P. aeruginosa* is PA01; wild-type *E. coli* is D21; wild-type *S. aureus* is ATCC #29213; wild-type *S. epidermidis* is ATCC #35984; wild-type *E. faecalis* is ATCC #29212. ^bDetermined by the broth microdilution method. ^cΔRND = mutation of *mexAB*, *mexCD*, *mexXY*, *mexHI*, *opmH*. ^dThese strains show a slight growth defect on agar medium. ND = Not determined

with ACC in toto and not just the isolated subunits, because the multiprotein complex is the active form of the enzyme in vivo.

The inhibition of ACC by moiramide B was determined by varying acetyl-CoA at increasing fixed concentrations of inhibitor, while ATP was held constant at a subsaturating level. Thus, compound 4 exhibited competitive inhibition versus acetyl-CoA with a K_{is} of 7.9 ± 1.1 nM (Figure 4D). These results are similar to the competitive inhibition pattern of 4 versus malonyl-CoA and the K_{is} value of 5 nM for the isolated subunit of CT.¹²

For the dual-ligands, inhibition patterns using biochemical assays were determined versus both ATP and acetyl-CoA. The inhibition of ACC by compound 5 (15C linker) versus ATP at increasing fixed concentrations of inhibitor, with acetyl-CoA held constant at a subsaturating level, exhibited noncompetitive inhibition with a K_{is} of 28.7 ± 12.9 nM and a K_{ii} of 33.7 ± 7.2 nM (Figure 4B). The inhibition of ACC by compound 5 versus acetyl-CoA at increasing fixed concentrations of inhibitor, with ATP held constant at a subsaturating level, exhibited competitive inhibition with a K_{is} of 5.2 ± 0.7 nM (Figure 4E).

The inhibition of ACC by compound 6 (7C linker) versus ATP at increasing fixed concentrations of inhibitor, with acetyl-CoA held constant at a subsaturating level, exhibited noncompetitive inhibition with a K_{is} of 16.9 ± 6.8 nM and a K_{ii} of 9.6 ± 1.0 nM (Figure 4C). The inhibition of ACC by dual-ligand 6 versus acetyl-CoA at increasing fixed concentrations of inhibitor, with ATP held constant at a subsaturating level, exhibited competitive inhibition with a K_{is} of 5.5 ± 0.6 nM (Figure 4F).

The noncompetitive inhibition pattern versus ATP and the competitive pattern versus acetyl-CoA observed for both 5 and 6 could be due to the linker not being long enough to allow both parts of the dual-ligands to bind to the enzyme simultaneously. As a consequence, compounds 5 and 6 could only bind in the moiramide B binding site, by virtue of its higher affinity, compared to compound 2. While this is a plausible explanation for the noncompetitive inhibition pattern versus ATP, it is inconsistent with the fact that the “parent” compound 2 also exhibited noncompetitive inhibition versus

ATP in ACC. Thus, the inhibition patterns for the compounds 5 and 6 are perfectly consistent with the inhibition patterns observed for the two “parent” compounds, 2 and 4. The molecular basis for the inhibition patterns will ultimately be revealed by the determination of the three-dimensional structure of ACC bound to either of the dual-ligands. Lastly, given that neither pharmacophore, compounds 2 nor 4, inhibits human ACC,^{10,12} it is unlikely that the dual-ligands would inhibit the human enzyme.

Antibacterial Activity of Dual-Ligands. Table 1 lists the minimum inhibitory concentration (MIC) values for the “parent” compounds 2 and 4, as well as compounds 5 and 6, against different bacterial strains. Compound 2 exhibited antibacterial activity against efflux-pump deficient *E. coli* and, in fact, registered the same MIC value of 16 μg/mL as reported by Mochalkin et al.¹⁰ Also consistent with the findings of Mochalkin et al., compound 2 was not active against any Gram-positive bacteria.¹⁰ Moreover, 2 was effective against an *E. coli tolC* derivative that was selected for spontaneous resistance to 4 suggesting that dual-ligands such as 6 would retain activity against strains bearing pre-existing moiramide resistance.

Compound 4 exhibited antibacterial activity against all strains tested except the wild-type strains of *Pseudomonas aeruginosa* and *E. coli*. The lack of activity against these strains can be attributed to efflux-based intrinsic resistance, since efflux-pump-deficient strains of these organisms were susceptible to 4 (Table 1). Compound 4 also exhibited activity against spontaneous moiramide-resistant isolates of both *E. coli tolC* and *Staphylococcus aureus*, with an observed 8-fold decrease in potency in each case. The elevated MICs against 4 suggest that some stable drug resistance was observed, most likely through a target-based spontaneous mutation. The results reported herein for 4 are consistent with previously reported antibacterial analyses.^{12,13,33}

Of the dual-ligands tested, compound 6 bearing the shorter 7C linker was found to exhibit the best overall antibacterial activity in MIC assays (Table 1). Antibacterial activity was observed against an efflux compromised *E. coli* strain lacking the *tolC* outer membrane channel and wild-type *S. aureus*. In fact, compound 6 was effective against all but one of the Gram-

positive strains investigated. Of particular note and, in contrast to 4, MIC values for 6 were unchanged at 4 $\mu\text{g}/\text{mL}$ when tested against wild-type *S. aureus* and an otherwise isogenic strain bearing a gain-of-function mutation³⁴ effecting *norA*-based efflux activity (compare MICs for compounds 4 and 6 versus wild-type and *norA*^{up} *S. aureus* in Table 1). From this, we conclude that compound 6 is no longer a substrate for NorA-based efflux in *S. aureus*; whereas, the parent compound 4 is appreciably impacted by a mutational gain-of-function of the NorA efflux pump. Such differential recognition of closely related antimicrobial substrates has been reported previously.³⁵ Compound 6 was also still effective against moiramide-resistant *E. coli tolC* but ineffective against moiramide-resistant *S. aureus*. This result is wholly expected given that the secondary pharmacophore (the aminooxazole derivative) is not effective against Gram-positive bacteria due to a threonine residue at position 437 of BC (which is an isoleucine in Gram-negative bacteria) causing a loss in necessary hydrophobic contacts between the inhibitor and the binding pocket.⁹ Lastly, while the antibacterial activity of 6 is slightly reduced (i.e., 4–8-fold) relative to 4 in most strains, there was an increase in potency for 6 with an MIC of 4 $\mu\text{g}/\text{mL}$ against *Enterococcus faecalis*, whereas 4 showed an MIC of 8 $\mu\text{g}/\text{mL}$. The absence of any apparent antibacterial activity of compound 5 is unexpected as 5 did, in fact inhibit the holoenzyme ACC. We speculated that compound 5 might be impaired in its ability to diffuse through the bacterial membrane due to the presence of the longer, hydrophobic linker.

Effect of PMBN on the Antibacterial Activity of Compound 5. Polymyxin B nonapeptide (PMBN) is a cationic cyclic peptide that is a non-bactericidal version of the antibiotic polymyxin B (PMB). PMBN binds to the bacterial lipopolysaccharide found in the outer membrane of Gram-negative bacteria which leads to increased susceptibility to the passage of hydrophobic antibiotics.^{36,37} Therefore, the effect of PMBN on the antibacterial activity of compound 5 was examined to determine whether or not an inability to diffuse across the bacterial membrane was the reason for the lack of observed antibacterial activity.

The antibacterial activity of 5 when co-incubated in *E. coli* with PMBN is shown in Figure 5. As expected, there was no antibacterial activity observed for 5 when inoculated in *E. coli* without PMBN. However, with increasing amounts of PMBN,

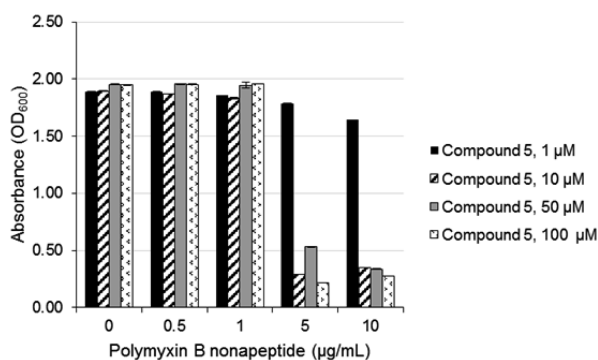


Figure 5. Effect of polymyxin B nonapeptide (PMBN) on the antibacterial activity of 5. Increasing amounts of PMBN (0, 0.5, 1, 5, 10 $\mu\text{g}/\text{mL}$) were added to different fixed concentrations of 5 (1, 10, 50, 100 μM). The solutions were inoculated with *E. coli* and incubated at 37 °C. After a 4 h incubation, the absorbance at 600 nm was measured.

compound 5 did inhibit bacterial growth (Figure 5). Concentrations of 10, 50, and 100 μM of compound 5 inhibited growth of *E. coli* when inoculated with at least 5 $\mu\text{g}/\text{mL}$ of PMBN. There was no significant inhibition of growth with only 1 μM of 5, even with the addition of PMBN. Control experiments showed no growth inhibition when *E. coli* was inoculated with only PMBN at the highest concentration (10 $\mu\text{g}/\text{mL}$) used in the assay (Supporting Information, Table S1). These results strongly suggest that the lack of antibacterial activity of compound 5, even at high concentrations, was due to an inability to diffuse across the bacterial membrane. Thus, the antibacterial activity of 5 in the presence of PMBN can be attributed to the ability of 5 to enter the cell and inhibit ACC. This result implies synergy between PMBN and compound 5 which can be beneficial when developing combination therapies targeting Gram-negative pathogens.^{38,39}

Single-Step Resistance Studies. One of the potential advantages of a dual-ligand antibacterial agent versus a molecule directed against a single target is a lower likelihood of developing resistance. To this end, the spontaneous resistance frequencies were determined for rifampin, 2, 4, and 6 against the *E. coli tolC* mutant (Table 2). Compared to the control

Table 2. Results of Single-Step Resistance Selection Studies with the *E. coli tolC* Strain

compound	MIC ^a (mg/L)	MPC ^b (mg/L)	MSW ^c	resistance frequency ^d
rifampin	8	>64	>8	7×10^{-9}
2	16	>128	>8	1.75×10^{-9}
4	0.5	16	32	$<2.5 \times 10^{-10}$
6	8	64	8	$<2.5 \times 10^{-10}$

^aDetermined from broth microdilution in MHII broth. ^bMPC is the drug dose at which resistant mutants (using 4×10^9 CFU) were no longer obtained. ^cMSW is the ratio of the MPC to the MIC. ^dResistance frequency is the number of resistant colonies observed over the total number of CFU plated at 8x MIC

rifampin, compound 2 had a lower frequency of resistance and, in general, was found to be a poor inhibitor in these assays. In contrast, the mutant prevention concentrations (MPC) for compounds 4 and 6 were 16 mg/L and 64 mg/L, respectively. This allowed for the calculation of mutant selection windows (MSWs) for these compounds where the MSW is the MPC:MIC ratio, with an ideal drug having an MSW of 1.⁴⁰ The MSW values for 4 and 6 were 32 and 8, respectively. Thus, even though 6 was somewhat lower in potency than the moiramide parent compound, the smaller MSW suggests it has more restriction for selection of resistance. This is a potentially exciting observation as compounds with a smaller MSW are far less likely to select for spontaneous resistance *in vivo* when dosed appropriately above their respective MPC.⁴¹ Lastly, when dosed at 8 times the MIC value, compounds 4 and 6 both exhibited an observed resistance frequency of $<2.5 \times 10^{-10}$. This number was too low to determine any significant difference between the two compounds. Therefore, it could not be assessed if 6 has a lower frequency of resistance when compared to the two “parent” compounds. Nonetheless, when compared to rifampin and 2, compound 6 clearly has a much lower potential for spontaneous resistance development.

CONCLUSIONS

The studies in this report provide “proof-of-concept” that a dual-ligand inhibitor of the multifunctional enzyme acetyl-CoA carboxylase can act as an antibacterial agent. First, the synthesis of the dual-ligand inhibitor led to significant improvements in the synthetic protocol for compound **4**. Second, incorporating two known inhibitors for the two enzymes comprising ACC, biotin carboxylase and carboxyltransferase, covalently attached via a linker into a single chemical entity yielded a potent (nM inhibition constant) inhibitor of the enzyme. However, based on our results, we speculate that the more hydrophobic the linker is, the less likely it is to diffuse across the bacterial membrane.

The original impetus for using a dual-ligand inhibitor of ACC as an antibacterial agent as opposed to using each pharmacophore individually (i.e., combination therapy) was that previous kinetic studies showed communication between the two active sites of the enzyme which implies a physical interaction between the proteins.²⁰ The design of these dual-ligand molecules was such that they act as stable, dual-pharmacophore agents and not as prodrugs. This strategy should ensure that the pharmacokinetics, pharmacodynamics, and tissue distribution of the composite pharmacophores are matched which may impart certain advantages over combination therapies involving the two parent agents alone. For example, while the potency of **4** is impacted by efflux-based exclusion in strains bearing a gain-of-function mutation in the gene encoding the *S. aureus* NorA efflux pump, compound **6** does not appear to be impacted by this activity suggesting it is no longer a substrate for NorA-based efflux. Further studies comparing the activity of this and other optimized moiramide B and aminooxazole dual-ligands relative to cocktails of the two parent agents will be the subject of future studies.

The observation that compound **6** exhibited a frequency of resistance that was less than 10^{-10} , whereas the frequency of resistance of single targets is between 10^{-6} to 10^{-9} ,¹⁹ bears out the dual-ligand approach described here. Most importantly, compound **6** had a smaller MSW than **4** indicating that a lower dose is needed to prevent the development of resistance bacteria. The smaller MSW for **6** vs **4** is also consistent with a role for the aminooxazole pharmacophore in the dual-ligand since narrower MSW values are expected for two intracellular targets compared to one target.⁴¹ All in all, the results suggest that a dual-ligand approach demonstrates the potential for antibacterial agents directed against ACC.

An unexpected but potentially far-reaching finding was that compound **2** exhibited noncompetitive inhibition of BC with respect to ATP in ACC, but competitive inhibition in the isolated BC subunit. This indicates that inhibitors of BC discovered using the isolated subunit may react differently with ACC. Third, the finding that compound **5** had little to no antibacterial activity, while **6** exhibited antibacterial activity against Gram-negative and Gram-positive organisms indicates that the choice of the linking component is critical for determining whether dual-ligand inhibitors which show activity in biochemical assays will also show antibacterial activity.

The choice of compound **2** as the BC inhibitor was a compromise between its relatively low affinity ($K_i = 400$ nM) and its synthetic tractability. Nonetheless, several lines of evidence suggest that it played a role in the antibacterial activity of the dual-ligands. While the pharmacophore involving parent compound **2** was not as potent as the parent compound **4**, it

did retain appreciable antibacterial activity in vitro. Nevertheless, in single-step resistance studies in vitro, compound **6** exhibits low resistance development potential and its MSW was 4 times smaller than that of the parent compound **4**. This strongly suggests that the secondary activity of **6** is antimicrobial, and, as is the case for other dual-targeting classes of antimicrobials (e.g., fluoroquinolones), may be a better indicator of the ability of this class of compounds to prevent spontaneous resistance development, rather than its overall potency.⁴¹

Nevertheless, while the pharmacophore involving compound **2** was not as potent as compound **4**, many novel aminooxazole derivatives were recently reported as part of a recent virtual screening study⁴² which identified several million aminooxazole derivatives that could potentially be linked to compound **4** to generate a wide array of dual-ligand hybrids. These new dual-ligands could, in turn, be screened for potent broad spectrum antibacterial activity using the tools and techniques described herein. Future studies will seek to test this proposal directly and will undoubtedly provide new and important information about the activity of dual-ligand inhibitors against this novel target.

EXPERIMENTAL SECTION

Materials and Methods. All chemicals and reagents were purchased from Sigma-Aldrich, Fisher, Acros, NovaBiochem, Matrix, Combi-Blocks, or Fluka and used without further purification. Diisopropylethylamine and triethylamine were dried and distilled from CaH₂ and stored over KOH pellets. Dry methanol was distilled from Mg turnings and stored over 3 Å molecular sieves. All reactions were performed under a dry nitrogen atmosphere unless otherwise noted. Flash chromatography was performed using 230–400 mesh silica gel (40–63 μm) from Sigma-Aldrich. RP-HPLC was performed with a Waters 616 pump, Water 2707 Autosampler, and 996 Photodiode Assay Detector which are controlled by Waters Empower 2 software. The linear gradient resulted from mixing eluents A (0.1% TFA in water) and B (0.1% TFA in acetonitrile). Method A: The separation was performed on an Agilent Zorbax 300 Extend-C18 (5 μm, 150 × 4.6 mm) with Agilent guard column Zorbax 300 SB-C18 (5 μm, 12.5 × 4.6 mm). Method B: The separation was performed on an Agilent Zorbax 300 SB-C18 (5 μm, 250 × 4.6 mm) with Agilent guard column Zorbax 300 SB-C18 (5 μm, 12.5 × 4.6 mm). The flow rate was 1.0 mL/min, and detected wavelength was 215 nm. Thin layer chromatography (TLC) was performed on aluminum-backed 60 F₂₅₄ silica plates from EMD Chemicals, Inc. Optical rotations were recorded on a Jasco P-2000 digital polarimeter. Circular dichroism (CD) spectrum was recorded on a Jasco J-815 circular dichroism spectrometer. ¹H and ¹³C NMR spectra were recorded at room temperature on a Bruker AV-400 or AV-500 spectrometer. All NMR experiments were performed in deuterated solvents, and the chemical shifts are reported in standard δ notation as parts per million, using tetramethylsilane (TMS), CDCl₃, DMSO-*d*₆, or acetone-*d*₆ as an internal standard for ¹H and ¹³C NMR, with coupling constants (*J*) reported in Hertz (Hz). High resolution mass spectrometry (HRMS) was carried out using an Agilent 6210 electrospray ionization-time-of-flight (ESI-TOF) mass spectrometer. Purity of final compounds was determined by HPLC analysis as being ≥95%.

(E)-4-[(Benzylideneamino)methyl]phenol (9). Benzaldehyde **7** (413 μL, 431 mg, 4.06 mmol, 1.00 equiv) was added to a suspension of 3 Å molecular sieves (150 mg/100 mg amine), triethylamine (736 μL, 534 mg, 5.28 mmol, 1.30 equiv), and 4-hydroxybenzylamine **8** (500 mg, 4.06 mmol, 1.00 equiv) in dry methanol (1.0 mL/100 mg amine) at room temperature under N₂. The mixture was stirred at room temperature for 18 h. The molecular sieves were removed by filtration through a pad of Celite, washing well with dry methanol, and the filtrate was concentrated in vacuo to give **9** as a light brown solid (556 mg, 65%).⁴³ ¹H NMR (DMSO-*d*₆, 400 MHz): δ 4.64 (s, 2H), 6.72 (d, *J* = 8.4 Hz, 2H), 7.11 (d, *J* = 8.4 Hz, 2H), 7.41–7.49 (m, 3H), 7.70–

7.81 (m, 2H), 8.44 (s, 1H), 9.33 (br s, 1H). ^{13}C NMR (DMSO- d_6 , 100 MHz): δ 64.1, 115.6, 128.4, 129.1, 129.6, 130.1, 131.1, 136.6, 156.7, 161.5. HRMS (ESI-TOF): calcd for $\text{C}_{14}\text{H}_{14}\text{NO}$ (M+H) $^+$, 212.1070; obsd, 212.1070.

4-[(Benzylamino)methyl]phenol (10). Sodium borohydride (154 mg, 4.06 mmol, 1.80 equiv) was added in portions to a solution of **9** (556 mg, 2.63 mmol, 1.00 equiv) in dry methanol (5 mL) at 0 °C. The mixture was stirred for 18 h under N_2 while allowing to warm to room temperature. The mixture was concentrated and then partitioned between CH_2Cl_2 (10 mL) and water (10 mL). The aqueous layer was further extracted with CH_2Cl_2 (2 \times 10 mL). The combined organic layers were washed with brine, dried over MgSO_4 , filtered, and concentrated to give **10** as a light brown solid (470 mg, 84%). R_f 0.27 (3:2 CH_2Cl_2 :EtOAc). ^1H NMR (acetone- d_6 , 400 MHz): δ 3.69 (s, 2H), 3.77 (s, 2H), 5.55 (s, 1H), 6.80 (d, J = 8.4 Hz, 2H), 7.19 (d, J = 8.4, 2H), 7.23 (d, J = 7.4 Hz, 1H), 7.30 (t, J = 7.4 Hz, 2H), 7.37 (d, J = 7.4 Hz, 2H). ^{13}C NMR (acetone- d_6 , 100 MHz): δ 52.2, 52.5, 115.3, 126.7, 128.2, 128.3, 129.5, 130.9, 140.7, 156.7. HRMS (ESI-TOF): calcd for $\text{C}_{14}\text{H}_{16}\text{NO}$ (M+H) $^+$, 214.1226; obsd, 214.1225.

2-Amino-oxazole-5-carboxylic Acid (12).¹⁰ Ethyl 2-amino-oxazole-5-carboxylate **11** (2.00 g, 12.8 mmol) was added to 2 M aqueous NaOH (50 mL) and stirred at room temperature for 2 h. The mixture was heated to 60 °C and stirred for an additional 2 h. Concentrated hydrochloric acid was added dropwise to the reaction mixture until it became acidic by pH paper (pH \sim 3–4) and a colorless precipitate began to form. The mixture was cooled in the freezer for 1 h. The resulting solid was collected by filtration and washed with acetonitrile to give **12** as a colorless solid (1.60 g, 98%). R_f 0.24 (6:4:1 CHCl_3 :MeOH:H $_2\text{O}$). ^1H NMR (DMSO- d_6 , 400 MHz): δ 7.38 (s, 2H), 7.44 (s, 1H). ^{13}C NMR (DMSO- d_6 , 100 MHz): δ 136.0, 137.1, 159.1, 164.1. HRMS (ESI-TOF): calcd for $\text{C}_4\text{H}_5\text{N}_2\text{O}_3$ (M+H) $^+$, 129.0295; obsd, 129.0296.

General Procedure for the Synthesis of Amino-oxazole Derivatives (2 and 13). Amine (1.00 equiv) was added to a solution of **12** (1.00 equiv) and triethylamine (2.00 equiv) in dry DMF (10 mL). HATU (1.00 equiv) was added to the solution and the mixture stirred for 20 h under N_2 . The mixture was partitioned between EtOAc (25 mL) and water (20 mL). The aqueous layer was further extracted with EtOAc (2 \times 20 mL). The combined organic layers were washed with saturated aqueous NaHCO_3 (15 mL) and brine (15 mL), dried over MgSO_4 , filtered, and concentrated. The resulting residue was dissolved in EtOAc (20 mL) and placed in a freezer overnight. The resulting precipitate was collected by filtration, washed with EtOAc, and dried.

2-Amino-*N,N*-dibenzyl-oxazole-5-carboxamide (2).¹⁰ Starting from dibenzylamine (249 μL , 256 mg, 1.30 mmol), carboxylic acid **12** (166 mg, 1.30 mmol), triethylamine (362 μL , 262 mg, 2.59 mmol), and HATU (493 mg, 1.30 mmol), the general procedure gave **2** as a colorless solid (124 mg, 31%). R_f 0.16 (3:2 CH_2Cl_2 :EtOAc). ^1H NMR (DMSO- d_6 , 400 MHz): δ 4.65 (br s, 4H), 7.06–7.41 (m, 13H). ^{13}C NMR (DMSO- d_6 , 100 MHz): δ 49.9, 52.5, 127.7, 128.5, 128.6, 129.1, 134.9, 137.4, 137.7, 159.0, 163.1. HRMS (ESI-TOF): calcd for $\text{C}_{18}\text{H}_{18}\text{N}_3\text{O}_2$ (M+H) $^+$, 308.1394; obsd, 308.1399.

2-Amino-*N*-benzyl-*N*-(4-hydroxybenzyl)-oxazole-5-carboxamide (13). Starting from amine **10** (1.20 g, 5.64 mmol), carboxylic acid **12** (721 mg, 5.64 mmol), triethylamine (1.57 mL, 1.14 g, 11.3 mmol), and HATU (2.14 g, 5.64 mmol), the general procedure gave **13** as a colorless solid (633 mg, 35%). R_f 0.57 (9:1 CH_2Cl_2 :MeOH). ^1H NMR (DMSO- d_6 , 400 MHz): δ 4.51 (s, 2H), 4.59 (s, 2H), 6.73 (d, J = 8.1 Hz, 2H), 7.42 (m, 10H), 9.40 (s, 1H). ^{13}C NMR (DMSO- d_6 , 100 MHz): δ 49.3, 115.8, 127.6, 129.1, 134.7, 137.5, 137.8, 157.1, 158.8, 163.1. HRMS (ESI-TOF): calcd for $\text{C}_{18}\text{H}_{18}\text{N}_3\text{O}_3$ (M+H) $^+$, 324.1343; obsd, 324.1371.

(4S)-Methylsuccinic Anhydride (15). Acetyl chloride (4.53 mL, 4.75 g, 60.6 mmol, 4.00 equiv) was added to (4S)-methylsuccinic acid **14** (2.00 g, 15.1 mmol, 1.00 equiv) and heated gently at reflux for 6 h. Excess acetyl chloride and acetic acid were removed in vacuo to give **15** as a colorless solid (1.70 g, 97%). R_f 0.76 (9:1 CH_2Cl_2 :MeOH). $[\alpha]_D^{24}$ –33.0 (c 1.77, CHCl_3) [Lit.²⁴ $[\alpha]_D^{24}$ –36.3 (c 1.77, CHCl_3)]. ^1H NMR (CDCl_3 , 400 MHz): δ 1.30 (d, J = 7.2 Hz, 3H), 2.45–2.56

(m, 1H), 2.99–3.17 (m, 2H). ^{13}C NMR (CDCl_3 , 100 MHz): δ 16.1, 35.6, 36.0, 169.9, 174.3. HRMS (ESI, -ve, TOF), calcd for $\text{C}_5\text{H}_8\text{O}_3$ (M-H) $^-$: 113.0244; obsd, 113.0244.

(4S)-Methyl-*N*-O-benzylsuccinimide (20).¹³ Triethylamine (1.08 mL, 787 mg, 7.78 mmol, 1.05 equiv) was added to a solution of **15** (845 mg, 7.41 mmol, 1.00 equiv) in CH_2Cl_2 (5 mL) at 0 °C followed by addition of *O*-benzylhydroxylamine hydrochloride **19** (1.24 g, 7.78 mmol, 1.05 equiv). The mixture was warmed to room temperature overnight under N_2 , and then 1,1'-carbonyldiimidazole (1.32 g, 8.15 mmol, 1.10 equiv) was added in portions. The mixture was stirred at room temperature for 1.5 h and then heated at reflux for 30 min. The mixture was cooled to room temperature, and the organic layer was washed with 10% hydrochloric acid (2 \times 10 mL). The organic layer was washed with brine (10 mL), dried over MgSO_4 , filtered, and concentrated to give **20** as a colorless solid (1.44 g, 89%). R_f 0.64 (4:1 EtOAc:Hex). $[\alpha]_D^{23}$ –2.0 (c 0.72, CHCl_3) [Lit.²⁴ $[\alpha]_D^{24}$ –4.9 (c 0.72, CHCl_3)]. ^1H NMR (CDCl_3 , 400 MHz): δ 1.25 (d, J = 7.2 Hz, 3H), 2.20 (dd, J = 17.5, 3.6 Hz, 1H), 2.67–2.80 (m, 1H), 2.82 (dd, J = 17.6, 8.9 Hz, 1H), 5.13 (s, 2H), 7.28–7.40 (m, 3H), 7.43–7.56 (m, 2H). ^{13}C NMR (CDCl_3 , 100 MHz): δ 16.7, 32.0, 33.7, 78.5, 128.5, 129.5, 130.1, 133.2, 170.6, 174.7. HRMS (ESI-TOF): calcd for $\text{C}_{12}\text{H}_{13}\text{NaNO}_3$ (M+Na) $^+$, 242.0788; obsd, 242.0804.

(3S)-Boc-L-valine-(4S)-methyl-*N*-O-benzylsuccinimide (21).^{13,24} A solution of Boc-L-valine (992 mg, 4.56 mmol, 1.00 equiv) and 1,1'-carbonyldiimidazole (814 mg, 5.02 mmol, 1.10 equiv) in dry THF (4 mL) was stirred at room temperature for 2 h under N_2 . A solution of **20** (1.00 g, 4.56 mmol, 1.00 equiv) in dry THF (8 mL) was added to the acylimidazole mixture at room temperature. This combined solution was then added dropwise over 45 min to a stirring solution of lithium hexamethyldisilazide (9.13 mL, 1.00 M, 9.13 mmol, 2.00 equiv) in dry THF (6 mL) under N_2 at –78 °C. After the addition was complete, the mixture was stirred at –78 °C for an additional 15 min and then quenched with saturated aqueous ammonium chloride (5 mL). The reaction mixture was allowed to warm to room temperature and then partitioned between Et $_2\text{O}$ (20 mL) and water (20 mL). The organic phase was washed with brine (20 mL), dried over MgSO_4 , filtered, and concentrated. The resulting residue was purified by flash chromatography on silica gel, eluting with 3:1 Hex:EtOAc, to give **21** as a colorless solid (800 mg, 42%). R_f 0.45 (2:1 Hex:EtOAc). $[\alpha]_D^{23}$ –30.1 (c 0.70, CHCl_3) [Lit.²⁴ $[\alpha]_D^{23}$ –33.9 (c 0.70, CHCl_3)]. ^1H NMR (CDCl_3 , 400 MHz): δ 0.78 (d, J = 6.7 Hz, 3H), 0.99 (d, J = 6.7 Hz, 3H), 1.23 (d, J = 7.4 Hz, 3H), 1.46 (s, 9H), 2.24–2.41 (m, 1H), 3.14–3.30 (m, 1H), 3.71 (d, J = 4.0 Hz, 1H), 4.44 (dd, J = 8.8, 4.8 Hz, 1H), 5.09 (s, 2H), 5.60 (d, J = 8.6 Hz, 1H), 7.30–7.39 (m, 3H), 7.40–7.46 (m, 2H). ^{13}C NMR (CDCl_3 , 100 MHz): δ 15.6, 17.3, 19.6, 28.3, 29.6, 34.5, 55.0, 65.1, 78.7, 80.2, 128.6, 129.6, 130.2, 132.9, 156.0, 166.6, 173.1, 201.9. HRMS (ESI-TOF): calcd for $\text{C}_{22}\text{H}_{30}\text{NaN}_2\text{O}_6$ (M+Na) $^+$, 441.1996; obsd, 441.1994.

(3S)-Boc-L-valine-(4S)-methylsuccinimide (22).²⁴ A catalytic amount of 5% Pd/C (127 mg, 20% w/w) was added to a solution of **21** (637 mg, 1.52 mmol, 1.00 equiv) in dry methanol (10 mL), and the mixture was stirred under H_2 for 1 h. The reaction mixture was filtered through a pad of Celite, washed with methanol, and concentrated. The residue was dissolved in acetonitrile (3 mL) and added dropwise to a stirred solution of 2-bromoacetophenone (303 mg, 1.52 mmol, 1.00 equiv) in acetonitrile (5 mL) at room temperature. A solution of triethylamine (318 μL , 231 mg, 2.28 mmol, 1.50 equiv) in acetonitrile (1 mL) was added dropwise over 2 h, and the reaction mixture was stirred at room temperature overnight. The mixture was concentrated and then partitioned between CH_2Cl_2 (25 mL) and 5% hydrochloric acid (2 \times 20 mL). The organic layer was washed with brine (20 mL), dried over MgSO_4 , filtered, concentrated, and purified by flash chromatography on silica gel eluting with 5:1 CH_2Cl_2 :EtOAc to give **22** as a yellow solid (303 mg, 64%). R_f 0.63 (3:1 CH_2Cl_2 :EtOAc). $[\alpha]_D^{24}$ –26.0 (c 1.005, CHCl_3) [Lit.²⁴ $[\alpha]_D^{23}$ –41.8 (c 0.66, CHCl_3)]. ^1H NMR (CDCl_3 , 400 MHz): δ 0.79 (d, J = 6.7 Hz, 3H), 1.02 (d, J = 6.7 Hz, 3H), 1.31 (d, J = 7.4 Hz, 3H), 1.45 (s, 9H), 2.15–2.23 (m, 1H), 3.14–3.22 (m, 1H), 3.93 (d, J = 5.3 Hz, 1H), 4.61 (dd, J = 9.0, 4.0 Hz, 1H), 5.80 (d, J = 9.2 Hz, 1H), 9.82 (s, 1H). ^{13}C NMR (CDCl_3 , 100 MHz): δ 15.3, 16.9, 19.7, 28.3, 29.7, 38.4, 59.0, 64.9, 80.3, 156.1,

172.1, 179.1, 202.2. HRMS (ESI-TOF): calcd for $C_{15}H_{24}NaN_2O_5$ ($M+Na$)⁺, 335.1577; obsd, 335.1582.

General Procedure for the Synthesis of Amines 23 and 25.²⁴

Trifluoroacetic acid (2.0 mL) was added dropwise to a solution of Boc-protected amine (**22** or **24**) (1.00 equiv) in CH_2Cl_2 (2.0 mL) at 0 °C, and stirring continued at 0 °C for 2 h, followed by the addition of toluene (10 mL) and removal of solvent in vacuo. The resulting residue was purified by flash chromatography on silica gel, with the less polar byproducts being flushed with 2–3 columns lengths of 1:1 CH_2Cl_2 :EtOAc and product being eluted with 9:1 CH_2Cl_2 :MeOH.

(3*S*)-*L*-Valine-(4*S*)-methylsuccinimide (**23**). Starting from Boc-protected amine **22** (200 mg, 0.64 mmol), the general procedure gave **23** as a light yellow foam (121 mg, 89%). R_f 0.50 (6:4:1 $CHCl_3$:MeOH:H₂O). HRMS (ESI-TOF): calcd for $C_{10}H_{16}N_2O_3$ ($M+H$)⁺, 213.1234; obsd, 213.1238.

(3*S*)- β -Phenylalanine-*L*-valine-(4*S*)-methylsuccinimide (**25**). Starting from Boc-protected amine **24** (183 mg, 0.398 mmol), the general procedure gave **25** as a light pink solid (141 mg, 98%). R_f 0.64 (6:4:1 $CHCl_3$:MeOH:H₂O). HRMS (ESI-TOF): calcd for $C_{19}H_{26}N_3O_4$ ($M+H$)⁺, 360.1918; obsd, 360.1927.

(3*S*)-*N*-Boc-3-amino- β -phenylalanine-*L*-valine-(4*S*)-methylsuccinimide (**24**).¹³ (*S*)-*N*-Boc-3-amino-3-phenylpropanoic acid (255 mg, 0.96 mmol, 1.20 equiv) was added to a solution of **23** (170 mg, 0.80 mmol, 1.00 equiv) in dry DMF (5.0 mL) at 0 °C. HATU (366 mg, 0.96 mmol, 1.20 equiv) was added to the solution, and stirring of the mixture began under N_2 . A solution of *N,N*-diisopropylethylamine (349 μ L, 259 mg, 2.00 mmol, 2.50 equiv) in dry DMF (1.5 mL) was added dropwise to the reaction over 1 h, while maintaining the temperature at 0 °C. The reaction was stirred for an additional 30 min at 0 °C before allowing the reaction mixture to warm to room temperature where stirring was continued for 20 h under N_2 . The solvent was removed in vacuo, and the mixture was partitioned between EtOAc (20 mL) and water (20 mL). The organic layer was washed with saturated aqueous $NaHCO_3$ (20 mL) and brine (20 mL), dried over $MgSO_4$, filtered, concentrated, and purified by flash chromatography on silica gel eluting with 3:2 Hex:EtOAc to give **24** as a colorless solid (166 mg, 45%). R_f 0.25 (1:1 Hex:EtOAc). $[\alpha]_D^{20}$ –53.2 (*c* 1.00, $CHCl_3$). ¹H NMR (DMSO-*d*₆, 400 MHz): δ 0.77 (d, *J* = 6.6 Hz, 3H), 0.85 (d, *J* = 6.6 Hz, 3H), 1.11 (d, *J* = 7.3 Hz, 3H), 1.34 (s, 9H), 2.23–2.37 (m, 1H), 2.42–2.50 (m, 1H), 2.71 (dd, *J* = 13.9, 9.3 Hz, 1H), 2.84–3.03 (m, 1H), 3.99 (d, *J* = 5.4 Hz, 1H), 4.71 (dd, *J* = 7.6, 5.3 Hz, 1H), 4.79–4.95 (m, 1H), 7.12–7.39 (m, 6H), 8.01 (d, *J* = 8.3 Hz, 1H), 11.37 (br s, 1H). ¹³C NMR (DMSO-*d*₆, 100 MHz): δ 15.0, 17.5, 20.0, 28.6, 28.8, 43.0, 52.1, 58.3, 63.4, 78.3, 126.6, 127.3, 128.7, 144.0, 155.0, 170.4, 174.2, 180.5, 203.7. HRMS (ESI-TOF): calcd for $C_{24}H_{34}N_3O_6$ ($M+H$)⁺, 460.2442; obsd, 460.2428.

Moiramide **B** (**4**). Sorbic acid (75 mg, 0.67 mmol, 1.20 equiv), TBTU (215 mg, 0.67 mmol, 1.20 equiv), and *N,N*-diisopropylethylamine (242 μ L, 180 mg, 1.39 mmol, 2.50 equiv) were added to a solution of **25** (200 mg, 0.56 mmol, 1.00 equiv) in dry DMF (2 mL), and the mixture was stirred for 20 h under N_2 . The mixture was partitioned between EtOAc (10 mL) and water (6 mL). The organic layer was washed with saturated aqueous $NaHCO_3$ (5 mL) and brine (5 mL), dried over $MgSO_4$, filtered, and concentrated. The resulting residue was purified by flash chromatography on silica gel eluting with 2% NH_4OH in 9:1 EtOAc:MeOH to give **4** as a colorless solid (81 mg, 32%).²⁴ R_f 0.54 (100% EtOAc). $[\alpha]_D^{24}$ –77.5 (*c* 1.00, MeOH) [Lit.²⁴ $[\alpha]_D^{25}$ –96.6 (*c* 0.28, MeOH)]. CD (*c* 1 μ M, MeOH) λ_{max} (theta) 213.0 (+9.68), 238.0 (–21.08), 292.0 (+0.69), 320.0 (–1.26). CD spectrum displayed λ_{max} values in good agreement with the literature though no concentrations were reported.^{17,24} ¹H NMR (DMSO-*d*₆, 400 MHz): δ 0.74 (d, *J* = 6.7 Hz, 3H), 0.79 (d, *J* = 6.7 Hz, 3H), 1.06 (d, *J* = 7.4 Hz, 3H), 1.77 (d, *J* = 6.4 Hz, 3H), 2.19–2.34 (m, 1H), 2.62 (dd, *J* = 14.1, 5.9 Hz, 1H), 2.76 (dd, *J* = 14.2, 8.7, 1H), 2.83–2.97 (m, 1H), 3.92 (d, *J* = 5.4 Hz, 1H), 4.62 (dd, *J* = 8.0, 5.6 Hz, 1H), 5.14–5.29 (m, 1H), 5.91 (d, *J* = 15.2, 1H), 6.06 (dq, *J* = 14.9, 6.8 Hz, 1H), 6.18 (dd, *J* = 14.9, 11.0 Hz, 1H), 6.94 (dd, *J* = 14.9, 11.0 Hz, 1H), 7.10–7.37 (m, 5H), 8.11 (d, *J* = 8.4 Hz, 1H), 8.41 (d, *J* = 8.4 Hz, 1H), 11.35 (br s, 1H). ¹³C NMR (DMSO-*d*₆, 100 MHz): δ 15.0, 17.7, 18.7, 19.9, 28.6, 39.5, 42.4, 50.3, 58.2, 63.5, 123.3, 126.9, 127.3, 128.6, 128.7, 130.3,

137.2, 139.9, 143.3, 164.9, 170.3, 174.2, 180.5, 203.8. HRMS (ESI-TOF): calcd for $C_{25}H_{32}N_3O_5$ ($M+H$)⁺, 454.2336; obsd, 454.2347.

General Procedure for the Synthesis of Alkyl Ester Linker Derivatives (27 and 30).²⁹

Concentrated sulfuric acid (2.00 equiv) was added to a solution of acid (1.00 equiv) in allyl alcohol. The solution was heated at reflux for 6 h. The mixture was cooled to room temperature, diluted with Et_2O (25 mL), and washed with saturated aqueous $NaHCO_3$ (2 \times 20 mL). The aqueous phase was back-extracted with Et_2O (15 mL). The combined organic layers were washed with brine (10 mL), dried over $MgSO_4$, filtered, and concentrated. The resulting oil was purified by flash chromatography on silica gel eluting with 4:1 Hex:EtOAc.

Allyl 16-Hydroxyhexadecanoate (**27**). According to the general procedure, concentrated sulfuric acid (391 μ L, 720 mg, 7.34 mmol), 16-hydroxyhexadecanoic acid **26** (1.00 g, 3.67 mmol), and allyl alcohol (35 mL) gave **27** as a colorless solid (704 mg, 61%). R_f 0.61 (1:1 Hex:EtOAc). ¹H NMR ($CDCl_3$, 400 MHz): δ 1.20–1.35 (m, 22H), 1.53–1.65 (m, 4H), 2.33 (t, *J* = 7.6 Hz, 2H), 3.64 (t, *J* = 6.6 Hz, 2H), 4.58 (d, *J* = 5.7 Hz, 2H), 5.24 (d, *J* = 10.4 Hz, 1H), 5.32 (d, *J* = 17.2 Hz, 1H), 5.92 (ddt, *J* = 17.2, 10.4, 5.7 Hz, 1H). ¹³C NMR ($CDCl_3$, 100 MHz): δ 24.9, 25.7, 29.1, 29.2, 29.4, 29.6, 32.8, 34.2, 62.9, 64.9, 118.0, 132.3, 173.5. HRMS (ESI-TOF): calcd for $C_{19}H_{36}NaO_3$ ($M+Na$)⁺, 335.2557; obsd, 335.2559.

Allyl 8-Hydroxyoctanoate (**30**). According to the general procedure, concentrated sulfuric acid (133 μ L, 245 mg, 2.50 mmol), 8-hydroxyoctanoic acid **29** (200 mg, 1.25 mmol), and allyl alcohol (8 mL) gave **30** as a yellow oil (148 mg, 59%). R_f 0.54 (1:1 Hex:EtOAc). ¹H NMR ($CDCl_3$, 400 MHz): δ 1.29–1.38 (m, 7H), 1.55 (p, *J* = 6.7 Hz, 2H), 1.64 (p, *J* = 6.9 Hz, 2H), 2.34 (t, *J* = 7.5 Hz, 2H), 3.61 (t, *J* = 6.6 Hz, 2H), 4.57 (d, *J* = 5.7 Hz, 2H), 5.23 (d, *J* = 10.4 Hz, 1H), 5.31 (d, *J* = 17.2 Hz, 1H), 5.92 (ddt, *J* = 17.2, 10.4, 5.7 Hz, 1H). ¹³C NMR ($CDCl_3$, 100 MHz): δ 24.8, 25.5, 28.9, 29.0, 32.6, 34.2, 62.7, 64.9, 118.1, 132.2, 173.5. HRMS (ESI-TOF): calcd for $C_{11}H_{20}NaO_3$ ($M+Na$)⁺, 223.1305; obsd, 223.1302.

General Procedure for the Synthesis of Iodoalkanoic Linker Derivatives 28 and 31.

Polymer-bound triphenylphosphine (100–200 mesh, polystyrene cross-linked with 2% divinylbenzene: ~3 mmol/g loading; 2.18 equiv) was suspended in dry CH_2Cl_2 (10 mL). Iodine (2.18 equiv) was added in portions until the dark color persisted. The mixture was stirred at room temperature under N_2 for 15 min. Imidazole (2.48 equiv) was added, and the reaction was stirred for an additional 15 min. A solution of compound **27** or **30** (1.00 equiv) in dry CH_2Cl_2 (5 mL) was added, and the mixture was heated at reflux for 30 min. The mixture was filtered to remove the resin and resin-bound byproducts, and the resin was washed with CH_2Cl_2 (15 mL). The filtrate was washed with saturated aqueous $Na_2S_2O_3$ (15 mL) and water (15 mL). The organic layer was dried over $MgSO_4$, filtered, and concentrated.

Allyl 16-Iodoheptadecanoate (**28**). Starting from polymer-bound triphenylphosphine (2.19 g, 8.36 mmol), iodine (2.12 g, 8.36 mmol), imidazole (647 mg, 9.51 mmol), and allyl ester linker **27** (1.20 g, 3.83 mmol), the general procedure gave **28** as a yellow solid (1.26 g, 78%). R_f 0.74 (2:1 Hex:EtOAc). ¹H NMR ($CDCl_3$, 400 MHz): δ 1.21–1.33 (m, 22H), 1.38 (p, *J* = 7.0 Hz, 2H), 1.62 (p, *J* = 7.0 Hz, 2H), 1.81 (p, *J* = 7.2 Hz, 2H), 2.31 (t, *J* = 7.5 Hz, 2H), 3.17 (t, *J* = 7.0 Hz, 2H), 4.56 (d, *J* = 5.6 Hz, 2H), 5.21 (d, *J* = 10.6 Hz, 1H), 5.30 (d, *J* = 17.1 Hz, 1H), 5.91 (ddt, *J* = 17.1, 10.6, 5.6 Hz, 1H). ¹³C NMR ($CDCl_3$, 100 MHz): δ 7.0, 24.9, 28.5, 29.1, 29.2, 29.4, 29.5, 29.6, 29.6, 30.5, 33.6, 34.2, 64.8, 117.9, 132.4, 173.2.

Allyl 8-Iodooctanoate (**31**). Starting from polymer-bound triphenylphosphine (394 mg, 1.50 mmol), iodine (382 mg, 1.50 mmol), imidazole (116 mg, 1.71 mmol), and allyl ester linker **30** (138 mg, 0.690 mmol), the general procedure gave **31** as a yellow oil (178 mg, 83%). R_f 0.48 (1:1 Hex:EtOAc). ¹H NMR ($CDCl_3$, 400 MHz): δ 1.22–1.33 (m, 7H), 1.40 (p, *J* = 6.6 Hz, 2H), 1.64 (p, *J* = 7.3 Hz, 2H), 1.82 (p, *J* = 7.2 Hz, 2H), 2.34 (t, *J* = 7.5 Hz, 2H), 3.18 (t, *J* = 7.0 Hz, 2H), 4.58 (d, *J* = 5.7 Hz, 2H), 5.24 (d, *J* = 10.4 Hz, 1H), 5.32 (d, *J* = 17.2 Hz, 1H), 5.92 (ddt, *J* = 17.2, 10.4, 5.7 Hz, 1H). ¹³C NMR ($CDCl_3$, 100 MHz): δ 7.2, 24.8, 28.2, 28.9, 30.3, 33.4, 34.1, 65.0, 118.1, 132.3, 173.3.

General Procedure for the Synthesis of Aminooxazole Conjugated to Linker Derivatives 32 and 33. Cesium hydroxide (1.00 equiv) was added to a solution of 13 (1.00 equiv) in dry DMF (5 mL). Linker derivative (28 or 31) (1.00 equiv) in dry THF (2 mL) was added to the reaction, and the mixture was heated at reflux for 24 h. Once cooled to room temperature, the mixture was filtered, and the precipitate was washed with THF. The solvent was removed in vacuo, the residue was partitioned between EtOAc (10 mL) and water (10 mL), and the organic layer was dried over MgSO₄, filtered, and concentrated.

Allyl 16-[4-[(2-Amino-N-benzyloxazole-5-carboxamido)methyl]phenoxy]hexadecanoate (32). Starting from cesium hydroxide (224 mg, 1.33 mmol), aminooxazole 13 (430 mg, 1.33 mmol), and linker 28 (562 mg, 1.33 mmol), the general procedure gave a residue that was purified by flash chromatography on silica gel eluting with 3:1 EtOAc:Hex that gave 32 as a pale yellow solid (166 mg, 20%). *R_f* 0.18 (3:1 EtOAc:Hex). ¹H NMR (CDCl₃, 400 MHz): δ 1.18–1.36 (m, 22H), 1.44 (p, *J* = 7.2 Hz, 2H), 1.63 (p, *J* = 6.9 Hz, 2H), 1.75 (p, *J* = 7.1 Hz, 2H), 2.32 (t, *J* = 7.5 Hz, 2H), 3.93 (t, *J* = 6.3 Hz, 2H), 4.53–4.68 (m, 6H), 5.22 (d, *J* = 10.4 Hz, 1H), 5.30 (d, *J* = 17.2 Hz, 1H), 5.91 (ddt, *J* = 17.2, 10.4, 5.7 Hz, 1H), 6.00 (br s, 2H), 6.85 (d, *J* = 7.9 Hz, 2H), 7.02–7.38 (m, 8H). ¹³C NMR (CDCl₃, 100 MHz): δ 25.0, 26.1, 29.1, 29.3, 29.5, 29.6, 29.7, 34.3, 49.1, 50.2, 64.9, 68.1, 114.8, 118.1, 127.6, 127.8, 128.5, 128.9, 132.3, 133.3, 138.1, 158.7, 159.5, 162.0, 173.6. HRMS (ESI-TOF): calcd for C₃₇H₅₂N₃O₅ (M+H)⁺, 618.3901; obsd, 618.3883.

Allyl 8-[4-[(2-Amino-N-benzyloxazole-5-carboxamido)methyl]phenoxy]octanoate (33). Starting from cesium hydroxide (257 mg, 1.53 mmol), aminooxazole 13 (494 mg, 1.53 mmol), and linker 31 (474 mg, 1.53 mmol), the general procedure gave a residue that was purified by flash chromatography on silica gel eluting with 4:1 EtOAc:Hex that gave 33 as a yellow oil (160 mg, 21%). *R_f* 0.43 (2.5:1 EtOAc:Hex). ¹H NMR (CDCl₃, 400 MHz): δ 1.25–1.52 (m, 7H), 1.65 (p, *J* = 6.8 Hz, 2H), 1.77 (p, *J* = 6.9 Hz, 2H), 2.34 (t, *J* = 7.5 Hz, 2H), 3.93 (t, *J* = 6.3 Hz, 2H), 4.48–4.69 (m, 6H), 5.22 (d, *J* = 10.4 Hz, 1H), 5.31 (d, *J* = 17.1 Hz, 1H), 5.90 (ddt, *J* = 17.1, 10.4, 5.4 Hz, 1H), 6.00 (br s, 2H), 6.85 (d, *J* = 8.0 Hz, 2H), 6.96–7.41 (m, 8H). ¹³C NMR (CDCl₃, 100 MHz): δ 24.9, 25.9, 29.0, 29.1, 29.2, 34.2, 49.2, 65.0, 68.0, 114.8, 118.2, 127.6, 128.9, 132.3, 133.3, 138.4, 158.7, 159.5, 161.7, 173.5. HRMS (ESI-TOF): calcd for C₂₉H₃₆N₃O₅ (M+H)⁺, 506.2649; obsd, 506.2656.

General Procedure for the Synthesis of Allyl Deprotected Aminooxazole-Linker Derivatives 34 and 35. A 2 M aqueous NaOH solution (5 mL) was added to a solution of aminooxazole-linker derivative 32 or 33 (1.00 equiv) in methanol (5 mL) and THF (2 mL), and the mixture was stirred at room temperature for 18 h. Concentrated hydrochloric acid was added dropwise to the reaction mixture until it became acidic by pH paper (pH ~3–4). The aqueous layer was extracted with EtOAc (3 × 10 mL), and the combined organic layers were washed with brine (6 mL), dried over MgSO₄, filtered, and concentrated.

16-[4-[(2-Amino-N-benzyloxazole-5-carboxamido)methyl]phenoxy]hexadecanoic Acid (34). Following the general procedure, compound 32 (89 mg, 0.144 mmol) gave 34 as a yellow solid (74 mg, 89%) that was taken into the next step without further purification. *R_f* 0.42 (4:1 EtOAc:Hex). HRMS (ESI-TOF): calcd for C₃₄H₄₈N₃O₅ (M+H)⁺, 578.3588; obsd, 578.3573.

8-[4-[(2-Amino-N-benzyloxazole-5-carboxamido)methyl]phenoxy]octanoic Acid (35). Following the general procedure, compound 33 (160 mg, 0.317 mmol) gave 35 as a yellow oil (104 mg, 71%) that was taken into the next step without further purification. *R_f* 0.23 (4:1 EtOAc:Hex). HRMS (ESI-TOF): calcd for C₂₆H₃₂N₃O₅ (M+H)⁺, 466.2336; obsd, 466.2324.

General Procedure for the Synthesis of Dual-Ligand Inhibitors 5 and 6. Amine 25 (1.00 equiv) was added to a solution of deprotected aminooxazole-linker (34 and 35) (1.20 equiv) and HATU (1.20 equiv) in dry DMF (3 mL) at 0 °C. *N,N*-Diisopropylethylamine (3.00 equiv) was added dropwise, and the reaction was stirred for an additional 30 min at 0 °C before allowing reaction to warm to room temperature where stirring was continued

for 20 h under N₂. The solvent was removed in vacuo, and the mixture was partitioned between EtOAc (10 mL) and water (10 mL). The organic layer was washed with 1 M hydrochloric acid (10 mL), saturated aqueous NaHCO₃ (10 mL), and brine (10 mL), dried over MgSO₄, filtered, concentrated.

Dual-Ligand Inhibitor with 15C-Linker (5). Starting from amine 25 (21 mg, 0.059 mmol), compound 34 (41 mg, 0.071 mmol), HATU (27 mg, 0.071 mmol), and *N,N*-diisopropylethylamine (31 μL, 23 mg, 0.178 mmol), the general procedure gave a residue that was purified by RP-HPLC (Method A: the gradient started from 30% B to 90% B in 40 min followed by 90% B to 95% B in 5 min and keeping at 95% for 10 min; retention time = 28.7 min) that gave 5 as a yellow solid (21 mg, 19%). *R_f* 0.70 (92:8 CH₂Cl₂:MeOH). [α]_D²⁴ –28.5 (c 0.425, MeOH). ¹H NMR (CD₃OD, 400 MHz): δ 0.79 (d, *J* = 6.7 Hz, 3H), 0.90 (d, *J* = 6.7 Hz, 3H), 1.16 (d, *J* = 7.3 Hz, 3H), 1.20–1.41 (m, 22H), 1.42–1.52 (m, 2H), 1.53–1.65 (m, 2H), 1.70–1.82 (m, 2H), 2.11–2.29 (m, 2H), 2.32–2.47 (m, 1H), 2.63–2.93 (m, 3H), 3.06–3.20 (m, 1H), 3.95 (t, *J* = 5.9 Hz, 2H), 4.63 (s, 2H), 4.68 (s, 2H), 4.76 (d, *J* = 4.5 Hz, 1H), 5.28–5.43 (m, 1H), 6.80–6.91 (m, 2H), 7.05–7.40 (m, 13H). HRMS (ESI-TOF): calcd for C₅₃H₇₁N₆O₈ (M+H)⁺, 919.5328; obsd, 919.5344.

Dual-Ligand Inhibitor with 7C-Linker (6). Starting from amine 25 (67 mg, 0.186 mmol), compound 35 (104 mg, 0.224 mmol), HATU (85 mg, 0.224 mmol), and *N,N*-diisopropylethylamine (97 μL, 72 mg, 0.559 mmol), the general procedure gave a residue that was purified by RP-HPLC (Method B: the gradient started from 20% B to 80% B in 30 min followed by 80% B to 95% B in 5 min and keeping at 95% for 10 min; retention time = 20.5 min) that gave 6 as a yellow solid (26 mg, 17%). *R_f* 0.59 (92:8 CH₂Cl₂:MeOH). [α]_D²⁴ –22.1 (c 1.17, MeOH). ¹H NMR (CD₃OD, 500 MHz): δ 0.74 (d, *J* = 6.7 Hz, 3H), 0.84 (d, *J* = 6.7 Hz, 3H), 1.11 (d, *J* = 7.4 Hz, 3H), 1.21–1.36 (m, 7H), 1.37–1.47 (m, 2H), 1.48–1.60 (m, 2H), 1.62–1.77 (m, 2H), 2.08–2.24 (m, 2H), 2.30–2.41 (m, 1H), 2.71–2.84 (m, 2H), 3.02–3.15 (m, 1H), 3.29 (s, 1H), 3.78–3.97 (m, 2H), 4.57 (s, 2H), 4.63 (s, 2H), 4.72 (d, *J* = 4.8 Hz, 1H), 5.24–5.39 (m, 1H), 6.83 (d, *J* = 7.4 Hz, 2H), 7.04–7.40 (m, 13H). HRMS (ESI-TOF): calcd for C₄₅H₅₅N₆O₈ (M+H)⁺, 807.4076; obsd, 807.4077.

Kinetic Assays. Acetyl-CoA carboxylase was purified according to Broussard et al. from a strain of *E. coli* that overexpresses the four genes that encode the enzyme.²⁰ The activity of ACC was determined spectrophotometrically by measuring the production of ADP using pyruvate kinase and lactate dehydrogenase and following the oxidation of NADH at 340 nm. Each reaction mixture contained 17.5 units of lactate dehydrogenase, 10.5 units of pyruvate kinase, 0.5 mM phosphoenolpyruvate, 0.2 mM NADH, 20 mM MgCl₂, 15 mM potassium bicarbonate, and 100 mM HEPES (pH 8.0). For reactions measuring the effects of inhibition versus ATP, each reaction contained a concentration of 0.2 mM acetyl-CoA, with ATP concentrations ranging from 0.8 μM to 56 μM. For reactions measuring the effects of inhibition versus acetyl-CoA, each reaction contained a concentration of 5 μM ATP, with acetyl-CoA concentrations ranging from 50 μM to 1000 μM. All reactions were conducted in a total of 0.5 mL in a 1 cm path length quartz cuvette, and all reactions were initiated by the addition of enzyme. Spectrophotometric data were collected using an Agilent Cary 60 UV–vis spectrophotometer interfaced with a personal computer with a data acquisition program.

Kinetic Analysis. Data were analyzed by nonlinear regression using the computer programs of Cleland.⁴⁴ Data describing competitive inhibition were fitted to eq 1, where *v* is the initial velocity, *V* is the maximal velocity, *A* is the substrate concentration, *K_m* is the Michaelis constant, *I* is the concentration of the inhibitor, and *K_{is}* is the slope inhibition constant.

$$v = \frac{VA}{K_m \left(1 + \frac{I}{K_{is}}\right) + A} \quad (1)$$

Data describing noncompetitive inhibition were fitted to eq 2, where *v* is the initial velocity, *V* is the maximal velocity, *A* is the substrate concentration, *K_m* is the Michaelis constant, *I* is the

concentration of the inhibitor, and K_{is} and K_{ii} are the slope and intercept inhibition constants, respectively.

$$v = \frac{VA}{K_m \left(1 + \frac{I}{K_{is}}\right) + A \left(1 + \frac{I}{K_{ii}}\right)} \quad (2)$$

Determination of MICs. Determination of MICs was conducted in accordance with the Clinical and Laboratory Standards Institute (CLSI) methodology using the broth microdilution methods with cation-adjusted Mueller Hinton (MHII) medium.⁴⁵ The strains tested were used with permission from the strain collection of TenNor Therapeutics. Test organisms were streaked onto agar medium and incubated overnight at 35 °C. Experimental compounds were tested over a concentration range prepared by 2-fold serial dilution after solubilizing compounds in 100% DMSO (or sterile water for gentamicin and kanamycin) to achieve a final stock concentration of 10 mg/L. A standardized inoculum of 5×10^5 CFU/mL in a volume of 0.1 mL was incubated with antibiotic for 18–24 h at 35 °C. The MIC was scored visually as the lowest concentration of antibiotic where no growth is apparent by visual inspection for turbidity.

Sensitization Assay using PMBN. A culture of *E. coli* strain JM109 was grown overnight in Luria broth (LB) at 37 °C. Culture tubes containing 2 mL of fresh LB media were inoculated with 10 μ L of the saturated *E. coli* culture. Polymyxin B nonapeptide (PMBN) was dissolved in water to achieve a 1 mM stock and inoculated into the tubes to generate final concentrations of 0.5, 1, 5, and 10 μ g/mL. Compound 5 was dissolved in 100% DMSO to achieve a 5 mM stock solution and inoculated into the tubes to generate final concentrations of 1, 10, 50, and 100 μ M. After inoculation, the culture tubes were incubated for 4 h at 37 °C. Optical density readings were measured at 600 nm in 1 mL plastic cuvettes. Spectrophotometric data were collected using an Agilent Cary 60 UV–vis spectrophotometer.

Generation of Spontaneous Resistant Mutant Strains and Resistance Studies. Single-step spontaneous resistance selections were undertaken on agar medium using overnight-saturated cultures grown in cation-adjusted Mueller Hinton (MHII). Briefly, compounds were added to molten MHII agar after allowing time to cool to 55 °C. Compounds were dosed in 2-fold increasing concentrations starting at 1 \times MIC. The test organism was grown overnight to saturation in MHII broth. The cells were concentrated by centrifugation, and the viable number of CFU plated was determined by serial dilution and plating. Each drug plate received a total of 4×10^9 CFU/plate (i.e., 0.1 mL plated of 4×10^{10} CFU/mL in the concentrated culture). Plates were monitored for the appearance of drug-resistant colonies. For selection of spontaneous moiramide resistance in the wild-type *S. aureus* and *E. coli tolC* backgrounds, moiramide was dosed at ~2–8 times their respective MICs, and potential drug-resistant isolates were evaluated after secondary passage through a drug-free intermediate. Stable moiramide resistance was verified by broth microdilution MIC assays, as above. The MPC was defined as the lowest consecutive drug concentration capable of fully suppressing the emergence of antibiotic-resistant bacterial subpopulations.⁴¹

■ ASSOCIATED CONTENT

● Supporting Information

¹H and ¹³C NMR spectra for compounds and supplemental figures and tables. This material is available free of charge via the Internet at <http://pubs.acs.org>.

■ AUTHOR INFORMATION

Corresponding Author

*E-mail: gwaldro@lsu.edu. Telephone: (225) 578-5209.

Notes

The authors declare no competing financial interest.

■ ACKNOWLEDGMENTS

The authors thank Dr. Jens Pohlmann for invaluable information on synthetic procedures and Dr. Zhenkun Ma at TenNor Therapeutics for the use of bacterial strains. The authors also thank Tyler Broussard for providing the ACC for kinetics studies and Dr. Ted Gauthier and the LSU AgCenter Biotechnology Laboratories for the collection of the CD spectrum.

■ ABBREVIATIONS USED

ACC, acetyl-CoA carboxylase; BC, biotin carboxylase; CT, carboxyltransferase; BCCP, biotin carboxyl carrier protein; MPC, mutant prevention concentration; MSW, mutant selection window; PMB(N), polymyxin B (nonapeptide)

■ REFERENCES

- (1) CDC. *Antibiotic Resistance Threats in the United States, 2013*; U.S. Department of Health and Human Services, Centers for Disease Control and Prevention: Atlanta, GA, 2013; <http://www.cdc.gov/drugresistance/threat-report-2013/>.
- (2) Heath, R. J.; Rock, C. O. Fatty acid biosynthesis as a target for novel antibacterials. *Curr. Opin. Investig. Drugs* **2004**, *5*, 146–153.
- (3) Zhang, Y. M.; White, S. W.; Rock, C. O. Inhibiting bacterial fatty acid synthesis. *J. Biol. Chem.* **2006**, *281*, 17541–17544.
- (4) Campbell, J. W.; Cronan, J. E., Jr. Bacterial fatty acid biosynthesis: targets for antibacterial drug discovery. *Annu. Rev. Microbiol.* **2001**, *55*, 305–332.
- (5) Cronan, J. E., Jr.; Waldrop, G. L. Multi-subunit acetyl-CoA carboxylases. *Prog. Lipid Res.* **2002**, *41*, 407–435.
- (6) Tanabe, T.; Wada, K.; Okazaki, T.; Numa, S. Acetyl-coenzyme-A carboxylase from rat liver. Subunit structure and proteolytic modification. *Eur. J. Biochem.* **1975**, *57*, 15–24.
- (7) Rock, C. O.; Cronan, J. E. *Escherichia coli* as a model for the regulation of dissociable (type II) fatty acid biosynthesis. *Biochim. Biophys. Acta* **1996**, *1302*, 1–16.
- (8) Heath, R. J.; White, S. W.; Rock, C. O. Inhibitors of fatty acid synthesis as antimicrobial chemotherapeutics. *Appl. Microbiol. Biotechnol.* **2002**, *58*, 695–703.
- (9) Miller, J. R.; Dunham, S.; Mochalkin, I.; Banotai, C.; Bowman, M.; Buist, S.; Dunkle, B.; Hanna, D.; Harwood, H. J.; Huband, M. D.; Karnovsky, A.; Kuhn, M.; Limberakis, C.; Liu, J. Y.; Mehrens, S.; Mueller, W. T.; Narasimhan, L.; Ogden, A.; Ohren, J.; Prasad, J. V.; Shelly, J. A.; Skerlos, L.; Sulavik, M.; Thomas, V. H.; VanderRoest, S.; Wang, L.; Wang, Z.; Whitton, A.; Zhu, T.; Stover, C. K. A class of selective antibacterials derived from a protein kinase inhibitor pharmacophore. *Proc. Natl. Acad. Sci. U.S.A.* **2009**, *106*, 1737–1742.
- (10) Mochalkin, I.; Miller, J. R.; Narasimhan, L.; Thanabal, V.; Erdman, P.; Cox, P. B.; Prasad, J. V.; Lightle, S.; Huband, M. D.; Stover, C. K. Discovery of antibacterial biotin carboxylase inhibitors by virtual screening and fragment-based approaches. *ACS Chem. Biol.* **2009**, *4*, 473–483.
- (11) Needham, J.; Kelly, M. T.; Ishige, M.; Andersen, R. J. Andrimid and moiramides A–C, metabolites produced in culture by a marine isolate of the bacterium *Pseudomonas fluorescens*: Structure elucidation and biosynthesis. *J. Org. Chem.* **1994**, *59*, 2058–2063.
- (12) Freiberg, C.; Brunner, N. A.; Schiffer, G.; Lampe, T.; Pohlmann, J.; Brands, M.; Raabe, M.; Habich, D.; Ziegelbauer, K. Identification and characterization of the first class of potent bacterial acetyl-CoA carboxylase inhibitors with antibacterial activity. *J. Biol. Chem.* **2004**, *279*, 26066–26073.
- (13) Pohlmann, J.; Lampe, T.; Shimada, M.; Nell, P. G.; Pernerstorfer, J.; Svenstrup, N.; Brunner, N. A.; Schiffer, G.; Freiberg, C. Pyrrolidinedione derivatives as antibacterial agents with a novel mode of action. *Bioorg. Med. Chem. Lett.* **2005**, *15*, 1189–1192.
- (14) The activity of carboxyltransferase is measured in the reverse or non-physiological direction where malonyl-CoA and biocytin (a biotin analogue) are the substrates. The formation of the product acetyl-CoA

- is detected using the coupling enzymes, citrate synthase and malate dehydrogenase: Blanchard, C. Z.; Waldrop, G. L. Overexpression and kinetic characterization of the carboxyltransferase component of acetyl-CoA carboxylase. *J. Biol. Chem.* **1998**, *273*, 19140–19145.
- (15) Li, S. J.; Cronan, J. E., Jr. Growth rate regulation of *Escherichia coli* acetyl coenzyme A carboxylase, which catalyzes the first committed step of lipid biosynthesis. *J. Bacteriol.* **1993**, *175*, 332–340.
- (16) Silver, L. L. Multi-targeting by monotherapeutic antibacterials. *Nat. Rev. Drug Discovery* **2007**, *6*, 41–55.
- (17) Pokrovskaya, V.; Baasov, T. Dual-acting hybrid antibiotics: a promising strategy to combat bacterial resistance. *Expert Opin. Drug Discovery* **2010**, *5*, 883–902.
- (18) O'Connell, K. M.; Hodgkinson, J. T.; Sore, H. F.; Welch, M.; Salmond, G. P.; Spring, D. R. Combating multidrug-resistant bacteria: Current strategies for the discovery of novel antibacterials. *Angew. Chem., Int. Ed.* **2013**, 10706–10733.
- (19) East, S. P.; Silver, L. L. Multitarget ligands in antibacterial research: progress and opportunities. *Expert Opin. Drug Discovery* **2013**, *8*, 143–156.
- (20) Broussard, T. C.; Price, A. E.; Laborde, S. M.; Waldrop, G. L. Complex formation and regulation of *Escherichia coli* acetyl-CoA carboxylase. *Biochemistry* **2013**, *52*, 3346–3357.
- (21) Li, H. Q.; Yan, T.; Yang, Y.; Shi, L.; Zhou, C. F.; Zhu, H. L. Synthesis and structure-activity relationships of *N*-benzyl-*N'*-(*X*-2-hydroxybenzyl)-*N''*-phenylureas and thioureas as antitumor agents. *Bioorg. Med. Chem.* **2010**, *18*, 305–313.
- (22) McWhorter, W.; Fredenhagen, A.; Nakanishi, K.; Komura, H. Sterecontrolled synthesis of andrimid and a structural requirement for the activity. *J. Chem. Soc., Chem. Commun.* **1989**, 299–301.
- (23) Rama Rao, A. V.; Singh, A. K.; Varaprasad, C. V. N. S. A convenient diastereoselective total synthesis of andrimid. *Tetrahedron Lett.* **1991**, *32*, 4393–4396.
- (24) Davies, S. G.; Dixon, D. J. Asymmetric syntheses of moiramide B and andrimid. *J. Chem. Soc., Perkin Trans. 1* **1998**, 2635–2643.
- (25) Fredenhagen, A.; Tamura, S. Y.; Kenny, P. T. M.; Komura, H.; Naya, Y.; Nakanishi, K.; Niegyama, K.; Sugiura, M.; Kita, H. Andrimid, a new peptide antibiotic produced by an intracellular bacterial symbiont isolated from a brown planthopper. *J. Am. Chem. Soc.* **1987**, *109*, 4409–4411.
- (26) Midgley, G.; Thomas, C. B. Selectivity of radical formation in the reaction of carbonyl-compounds with manganese (III) acetate. *J. Chem. Soc., Perkin Trans. 2* **1987**, 1103–1108.
- (27) Bailey, P. D.; Morgan, K. M.; Smith, D. I.; Vernon, J. M. Spiro cyclisations of *N*-acyliminium ions involving an aromatic π -nucleophile. *Tetrahedron Lett.* **2003**, *59*, 3369–3378.
- (28) Robin, S.; Zhu, J.; Galons, H.; Pham-Huy, C.; Claude, J. R.; Tomas, A.; Viosat, B. A convenient asymmetric synthesis of thalidomide. *Tetrahedron: Asymmetry* **1995**, *6*, 1249–1252.
- (29) Aron, Z. D.; Overman, L. E. Total synthesis and properties of the crambescidin core zwitterionic acid and crambescidin 359. *J. Am. Chem. Soc.* **2005**, *127*, 3380–3390.
- (30) Jobron, L.; Hummel, G. Solid-phase synthesis of new S-glycoamino acid building blocks. *Org. Lett.* **2000**, *2*, 2265–2267.
- (31) Zhang, Q.; Wu, Y.; Wang, L.; Hu, B.; Li, P.; Liu, F. Effect of hapten structures on specific and sensitive enzyme-linked immunosorbent assays for *N*-methylcarbamate insecticide metolcarb. *Anal. Chim. Acta* **2008**, *625*, 87–94.
- (32) Bennett, B. D.; Kimball, E. H.; Gao, M.; Osterhout, R.; Van Dien, S. J.; Rabinowitz, J. D. Absolute metabolite concentrations and implied enzyme active site occupancy in *Escherichia coli*. *Nat. Chem. Biol.* **2009**, *5*, 593–599.
- (33) Freiberg, C.; Pohlmann, J.; Nell, P. G.; Endermann, R.; Schuhmacher, J.; Newton, B.; Otteneder, M.; Lampe, T.; Habich, D.; Ziegelbauer, K. Novel bacterial acetyl coenzyme A carboxylase inhibitors with antibiotic efficacy *in vivo*. *Antimicrob. Agents Chemother.* **2006**, *50*, 2707–2712.
- (34) Robertson, G. T.; Bonventre, E. J.; Doyle, T. B.; Du, Q.; Duncan, L.; Morris, T. W.; Roche, E. D.; Yan, D.; Lynch, A. S. In vitro evaluation of CBR-2092, a novel rifamycin-quinolone hybrid anti-biotic: microbiology profiling studies with staphylococci and streptococci. *Antimicrob. Agents Chemother.* **2008**, *52*, 2324–2334.
- (35) Aeschlimann, J. R.; Dresser, L. D.; Kaatz, G. W.; Rybak, M. J. Effects of NorA inhibitors on *in vitro* antibacterial activities and postantibiotic effects of levofloxacin, ciprofloxacin, and norfloxacin in genetically related strains of *Staphylococcus aureus*. *Antimicrob. Agents Chemother.* **1999**, *43*, 335–340.
- (36) Viljanen, P.; Vaara, M. Susceptibility of Gram-negative bacteria to polymyxin B nonapeptide. *Antimicrob. Agents Chemother.* **1984**, *25*, 701–705.
- (37) Tsubery, H.; Ofek, I.; Cohen, S.; Eisenstein, M.; Fridkin, M. Modulation of the hydrophobic domain of polymyxin B nonapeptide: effect on outer-membrane permeabilization and lipopolysaccharide neutralization. *Mol. Pharmacol.* **2002**, *62*, 1036–1042.
- (38) Zavascki, A. P.; Goldani, L. Z.; Li, J.; Nation, R. L. Polymyxin B for the treatment of multidrug-resistant pathogens: a critical review. *J. Antimicrob. Chemother.* **2007**, *60*, 1206–1215.
- (39) Velkov, T.; Roberts, K. D.; Nation, R. L.; Wang, J.; Thompson, P. E.; Li, J. Teaching 'old' polymyxins new tricks: new-generation lipopeptides targeting Gram-negative 'superbugs'. *ACS Chem. Biol.* **2014**, *9*, 1172–1177.
- (40) Zhao, X.; Drlica, K. Restricting the selection of antibiotic-resistant mutant bacteria: measurement and potential use of the mutant selection window. *J. Infect. Dis.* **2002**, *185*, 561–565.
- (41) Drlica, K. The mutant selection window and antimicrobial resistance. *J. Antimicrob. Chemother.* **2003**, *52*, 11–17.
- (42) Brylinski, M.; Waldrop, G. L. Computational redesign of bacterial biotin carboxylase inhibitors using structure-based virtual screening of combinatorial libraries. *Molecules* **2014**, *19*, 4021–4045.
- (43) No R_f was obtained for imine compound as product hydrolyzed on silica.
- (44) Cleland, W. W. Statistical analysis of enzyme kinetic data. *Methods Enzymol.* **1979**, *63*, 103–138.
- (45) Clinical and Laboratory Standards Institute. Methods for dilution antimicrobial susceptibility tests for bacteria that grow aerobically, approved standard, 7th ed.; Clinical and Laboratory Standards Institute: Wayne, PA, 2006; CLSI document M7-A7, Vol. 26, no. 2.